Preparation and Determination of Rheological Behaviour of Fine Strontium Titanate Powder Suspensions

By

Uğur ÜNAL

A Dissertation Submitted to the
Graduate School in Partial Fulfillment of the
Requirements for the Degree of

MASTER OF SCIENCE

Department: Materials Science and Engineering
Major: Materials Science and Engineering

Izmir Institute of Technology
Izmir, Turkey

September , 1999

We approve the thesis of Uğur ÜNAL

Date of Signature

.....

Prof. Dr. Muhsin ÇİFTÇİOĞLU **29.09.1999**

Supervisor

Department of Chemical Enginnering

.....

Assist. Prof. Dr. Hurriyet POLAT **29.09.1999**

Department of Chemistry

.....

Assist. Prof. Dr. Funda TIHMINLIOĞLU **29.09.1999**

Department of Chemical Engineering

.....

Prof. Dr. Muhsin ÇİFTÇİOĞLU **29.09.1999**

Supervisor

Head of Interdisciplinary Materials Science and Engineering Program

ACKNOWLEDGEMENTS

I would like to thank to Prof. Dr. Muhsin Çiftçioğlu for his supervision, help, support and encouragement he provided during this project.

I also would like to thank to Assist. Prof. Dr. Mustafa Güden and Assist. Prof. Dr. Hürriyet Polat for their valuable comments and suggestions.

Special thanks are to all research assistants who helped me during the experimental work, for their friendships, and to the laboratory technicians Şerife Şahin and Nilgün Özgül for their help in the laboratory work.

I am very grateful for the help of Mr. Tamer Çakıcı from Politek Inc., Izmir, Turkey in the design and construction of the special set-up for electrorheological experiments.

Finally, I would like to thank to my family for their help, support and patience.

ABSTRACT

In this project, strontium titanate powders were prepared by using sol-gel and Pechini methods. In sol-gel method, the powders were prepared by mixing the TiO_2 sol and $Sr(NO_3)_2$ solution. Precipitation was observed after the addition of $Sr(NO_3)_2$ solution. Two powders were prepared by each method. In sol-gel method, acid:alcohol ratio was changed. In Pechini method, 50% of citric acid was substituted with polyacrylic acid. The characterization of the powders were performed by Fourier Transform Infrared Spectrophotometer (FTIR), Thermogravimetric Analyzer (TGA), Scanning Electron Microscope (SEM), X-Ray Diffraction and Optical Microscope.

The calcination temperature of 650 ^{0}C was chosen for sol-gel powder according to TGA data. XRD pattern showed that this temperature was not high enough to form complete $SrTiO_3$ phase, but no peaks related to nitrates or organic groups was observed in FTIR spectra. Sintering studies indicated that the agglomeration of sol-gel powder was very strong because the relative densities were very small. Pechini powders had weaker agglomerates and sintered to higher densities. The diameters of the Pechini powders were found as in the range of 0.2-0.5 μm.

The powders were dispersed in white oil and the rheological behaviour of these dispersions was studied by a rheometer. Several runs at different shear rates, and volume fractions were done. The suspensions without surfactant showed shear-thinning behavior, which indicates that the suspensions were flocculated. The addition of surfactant in certain amount produced stabilized suspensions. The stabilized suspensions showed Newtonian or Dilatant behaviour. The increase in the solids loading did not show significant change in the viscosity of stabilized suspension.

ÖZ

Bu projede, strontium titanate tozu sol-gel ve Pechini metodları kullanılarak yapılmıştır. Sol-gel metodunda, tozlar TiO_2 solu ve $Sr(NO_3)_2$ solüsyonu karıştırılarak üretilmiştir. $Sr(NO_3)_2$ solüsyonunun eklenmesinden sonra çökelme gözlenmiştir. Her iki yöntemle de ikişer toz üretilmiştir. Sol-gel metodunda, asit:alkol oranı değiştirilmiştir. Pechini metodunda, sitric acitin % 50 si poliakrilik asit ile değiştirilmiştir. Tozların karakterizasyonları termal gravimetrik analiz (TGA) cihazı, Fourier değişimli infrared spektra (FTIR), XRD, taramalı elektron mikroskopu (SEM) ve optik mikroskop kullanılarak yapıldı.

TGA verilerine dayanarak, sol-gel tozu için kalsinasyon sıcaklığı 650 ^0C olarak seçilmiştir. XRD sonuçları, bu sıcaklığın $SrTiO_3$ fazının tamamı ile oluşması için yeterli olmadığını göstermiş, ancak FTIR spektralarında nitrat ve organik piklerine rastlanmamıştır. Sinterleme çalışmaları, sol-gel tozunda çok kuvvetli topaklanmalar olduğunu göstermiştir. Sol-gel tozlarının relatif yoğunlukları sinterlemeden sonra dahi çok düşüktür. Pechini tozları daha zayıf topaklanmalara sahiptir ve sinterlemeden sonra daha yüksek relatif yoğunluklar göstermiştir. Pechini tozlarının çapları 0.2-0.5 μm arasında bulunmuştur.

Üretilen toz değişik yüzdelerde, pirinç yağının içinde dağıtılarak, katı yüzdesinin reolojik davranış üzerindeki etkisi araştırıldı. Bunun için bir rheometre kullanıldı. Farklı kayma gerilimlerinde ve hacimsel toz fraksiyonlarında çalışmalar yapılmıştır. Kararlı olmayan süspansiyonlar kayma gerilimi arttıkça viskozitede azalma göstermiştir, bu da topaklanmalara işaret eder. Ancak yüzey aktif maddesi eklendikten sonra, süspansiyonlar kararlı hale gelmiş ve dilatant ya da Newtonian davranış göstermişlerdir. Katı yüzdesindeki artış, kararlı haldeki süspansiyonlar için viskozitede çok büyük değişiklik yapmamıştır.

TABLE OF CONTENTS

LIST OF TABLES

LIST OF FIGURES

CHAPTER I

INTRODUCTION

Strontium titanate, which has a perovskite type of structure, has an increased attraction in recent years because of its unique properties such as high dielectric constant, high dielectric breakdown strength, chemical and thermal stability. Its dielectric constant is around 300 at room temperature and was studied by many workers. Hari Krishna Varma et. al. [42] investigated the change in the dielectric constant of strontium titanate due to the frequency of applied electric field. They have found that the dielectric constant of strontium titanate sintered at 1450 ^{0}C rises from 261 at 10^2 Hz to 249 at 10^7 Hz. Budd and Payne [4] also studied the change in the dielectric constant due to the variation of the amount of the tungsten. These studies showed that the increase in the amount of the tungsten caused a rise in the dielectric constant from 3100 upto 40,000 based on Internal Boundary Layer (IBL) capacitor.

Strontium titanate finds wide range of application areas with regarding to its convenient properties. Cell capacitors in DRAMs, Internal Boundary Layer (IBL) capacitors, varistors, oxygen sensors, and as a substrate for high T_C superconductors, etc. The appropriateness of strontium titanate powder for Internal Boundary Layer capacitors was investigated by Budd and Payne [4] and Fujimoto and Kingery [14].

Several types of methods are available for the preparation of fine dielectric ceramic powders. Conventional methods such as mixed oxide and coprecipitation methods are most widely used methods. However, these methods have some disadvantages compared to chemical methods. The conventional methods do not ensure the high purity of the end product and controlling the morphology of powder. Mixed oxide method simply involves the mixing of the salts of desired cations and calcination of the mixture at high temperatures. Fujimoto and Kingery [14] has studied the preparation of $SrTiO_3$ powder by

mixing oxide method. The calcination temperature of the mixture of $SrCO_3$ and TiO_2 with some additives were 1000 ^{0}C.

However, chemical methods such as sol-gel and Pechini methods permit to control the morphology of powder. Homogenous mixing of cations at molecular level ensures the high purity of powder. Controlling the reaction parameters allows to prepare ceramic powders with desired properties. Sol-gel and Pechini methods require low calcination temperatures. These methods yield excellent stoichiometry, low trace impurity content, fine particle size and homogenous particle distribution.

Sol-gel method is basically hydrolization of metal alkoxides in the presence of alcohol and acid. Hari Krishna Varma et. al. [42] have studied the preparation of $SrTiO_3$ by sol gel method. Titanium isopropoxide was hydrolyzed in the presence of isopropyl alcohol and acidic acid. The calcination temperature was between 250 and 1200 ^{0}C. The average aggregate size was 0.6 μm and above 98% of theoretical density is obtained at sintering temperature of 1450 ^{0}C.

In Pechini method, alpha carboxylic acids (citric acid, polyacrylic acid) form chelates with metal atoms (titanium, zirconium, etc.). Heating of the chelated product in the presence of polyhydroxy alcohol (ethylene glycol) leads to polyesterification and further heating results in black ash which yields powder when calcined at 400-600 ^{0}C [4,9,32].

Steven L. Peschke [32] studied the preparation of strontium titanate by Pechini method. In this study, the original Pechini method was modified and the effect of the substitution of citric acid with poly acrylic acid in various ratios was examined. According the Thermal Gravimetric Analyses of intermediate precursors, different calcination temperatures and their effect on particle morphology were studied. It was calculated that the particle diameter was 329 A for the powders formulated by 50%CA/50%PAA and calcined at 400 ^{0}C/600 ^{0}C. The particle diameter for 100% CA formulated powders was 659 A at

calcination temperatures of 550 ^{0}C/700 ^{0}C. SEM analyses of these powders exhibited that the average agglomerate sizes were 0.2-0.7 μm and particle sizes were in the range of 400-800 A in diameter.

Budd and Payne [4] used Pechini method to prepare W-doped $SrTiO_3$ powders. The average particle sizes of the powders calcined at 500 ^{0}C were less than 0.3 μm.

Electrorheology studies the change in the flow properties of dispersions of polarizable particles in an insulating oil under an applied electric field. Electrorheological phenomenon was first described by W.M. Winslow in 1949. His observations were on the change of the flow properties of starch, lime and silica dispersions in oil under an applied electric field. He has found that the dispersion shows resistance to flow when an electric field is applied [1, 2, 15].

Electrorheological fluids are composed of polarizable particles dispersed in nonconductive oil. Under applied electric field, dispersed particles are arranged due to the interactive forces among them and form chain or fiber like structure. The response of particles to the electric field is very short, in miliseconds and the process is reversible. The suspension takes its original state after the removal of electric field. The forces forming the chain are very strong, thus the deformation of the chain takes place at very high shear stresses. In some cases, the fibrillation or chain formation does not come up as reported by Kelly and Block. Bowen also reported the late fibril formation of $SrTiO_3$ particles after applying the electric field [2, 11, 12, 17, 18, 20, 22, 23, 43].

There are several parameters such as particle diameter and properties, particle concentration, electric field, properties of suspending oil and additives having an effect on the electrorheological phenomenon. Several types of materials were examined in different types of suspending medium. Block and Kelly [2] listed some formulation of electrorheological fluid dispersions.

Bowen et al. [3] investigated the electrorheological behaviour of $SrTiO_3$ suspensions in different types of polymer matrix materials. They observed that

suspensions in different types of polymer matrix materials. They observed that the strength of electrorheological effect increases with the concentration of particles and applied electric field. They also observed that ac field at frequency of 10 Hz exhibits stronger effect than when ac field at frequency of 100 Hz or dc field is applied.

Zhang et al. [47] dispersed $SrTiO_3$ particles in the size range of 0.5-10 μm in silicon oil and studied the electric field and temperature dependence of shear stress. They reported that shear stress at 2.4 kV/mm was 250 times of that without electric field. The shear stress was approximately proportional to the square of the electric field.

The objective of this study is to prepare stable dispersion of fine strontium titanate ceramic powder. Pechini and sol-gel methods have been used as preparation methods. The suspensions of $SrTiO_3$ powder have been prepared in white oil. The rheological behaviour of these suspensions has been investigated at different volume fractions and shear rates.

CHAPTER II

ELECTRICAL PROPERTIES OF ELECTRONIC CERAMICS

Ceramic materials have a wide range of electrical properties and are used in many electronic applications because of their unique, convenient electrical properties. The electrical properties of ceramic materials are improved by developed preparation techniques. There are varieties of electronic ceramics today. For example, porcelains and glasses were used as dielectric applications initially. However, in recent years new dielectric ceramics with higher dielectric constant and wider temperature range were developed with new techniques. Classification of electronic ceramics is given in Figure 2.1.

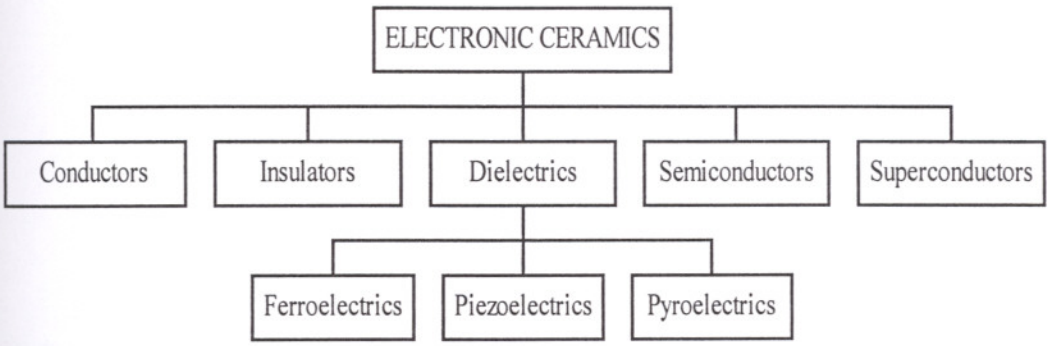

Figure 2.1. Classification of electronic ceramics

Different materials have different capabilities to conduct an electrical charge, when an electric field is applied. Most metals, some ceramics, and a few organics fall in this category for the reason that they have high electrical conductivity. These types of materials are called electrical conductors. Other materials that have very low conductivity such as most ceramics and organics are cited as electrical insulators [35].

Electrons flow through a wire when a potential difference is applied (Figure 2.2). The flow of electrons is referred to as current, which is inversely

proportional to the resistance of wire. The relation among the current, the voltage difference and the resistance is given by Ohm's law as below:

$$V = I.R \tag{2.1}$$

where V is the volt, I is the current and R is the resistance. The resistance of a material is dependent on the shape and a material constant called the electrical resistivity, that is,

$$R = \rho \frac{l}{A}; \tag{2-2}$$

ρ=electrical resistivity.

The reciprocal of electrical resistivity gives the conductivity;

$$\sigma = \frac{1}{\rho}; \tag{2-3}$$

σ= electrical conductivity.

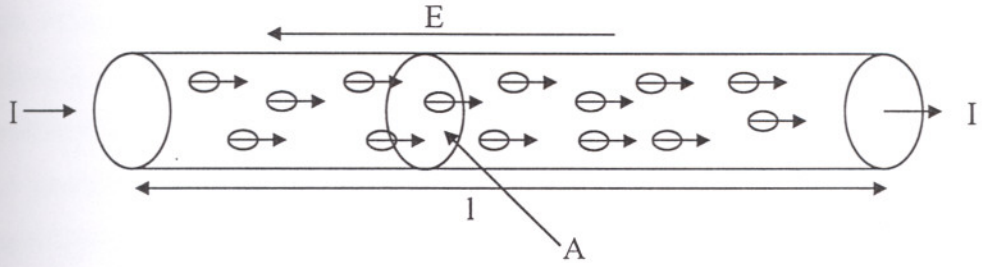

Figure 2.2. Flow of electrons in a conductor in the presence of an applied electric field.

Electrical resistivities of some materials are listed in Table 2.1. Electrical conductivity is determined by the number of charge carriers (n), the charge carried by each carrier (q), and the mobility of the carriers (μ) as expressed below;

$\sigma = nq\mu$.

The units are

$$\frac{1}{ohm.cm} = \left(\frac{carriers}{cm^3}\right)\left(\frac{coulombs}{carrier}\right)\left(\frac{cm/\sec}{volts/cm}\right)$$

There are two major mechanisms of electrical conductivity. One is electronic conductivity and the other is ionic conductivity. Metals are the most widely recognized materials having electronic conduction and have several types of crystal structures in which the metal atoms are bound together with their outer valence electrons by metallic bonding. These valence electrons are delocalized in the metallic structure. They are shared by many atoms and are not bound to any particular atom. These valence electrons are called charge carriers, which have an important role on the conductivity of materials. These charge carriers are accelerated, when an electric field is applied and move in opposite direction of electric field [19, 35].

A second major mechanism of electrical conductivity in materials is ionic conductivity. In this case, ions carry the electrical charges. Therefore, ionic conductivity is observed in the materials having ionic bonding. Electrons are relatively free to move in a metallic conductor under the influence of an electric field, but the movement of ions is limited in a crystal structure. Each positive ion is surrounded by negative ions and each negative ion is surrounded by positive ions. The overall charge is balanced and all the ions are in state of equilibrium. An additional energy is given to supply the movement of an ion. Ionic conductivity for a specific material arises at the point where the ions of the material gain sufficient thermal energy to overcome the energy barrier under the influence of electric field. Ionic conductivity is affected by many factors. Ionic conductivity increases as the temperature increases. An ion must have alternative positions to move into and must not alter the overall charge balance by the movement [19, 35].

Table 2-1. Electrical resistivities of some metals, polymers, and ceramics at room temperature [35].

Material	Resistivity (ohm-cm)
Copper	1.7×10^{-6}
Iron	10×10^{-6}
Tungsten	5.5×10^{-6}
Gold	2.4×10^{-6}
Ge	40
Diamond	1×10^{14}
SiO_2	$>10^{14}$
Fire-clay brick	10^{8}
Al_2O_3	$>10^{14}$
Teflon	10^{16}
Nylon	10^{14}

Some ceramic materials exhibit ionic conductivity. These ceramics are halides and chalcogenides of silver and copper where the metal atoms are disordered over several sites, oxides of the fluorite structure doped to cause a high concentration of oxygen vacancies and oxides with the beta-alumina structure that contain large structural channels through which monovalent cations can move. Varieties of applications of ionically conductive ceramics are based on oxygen ion conduction through doped ZrO_2. These applications include oxygen sensors, the oxygen pump, electrolysis, SO_x-NO_x decomposition, and the solid oxide fuel cell.

Most ceramic materials do not conduct or transmit electric current since they do not have mobile electrons or ions. This type of ceramic material is called electrical insulator. The resistivity of a ceramic material is temperature and impurity dependent and decreases with the increasing temperature and the amount of impurities [35].

Electrical insulators are used to isolate all electrical circuits. Ceramics are used where high strength, elevated temperature, heat dissipation or long

term hermecity (scaled from exposure to the atmosphere) are required. Among the applications of ceramic electrical insulators are integrated circuit chip carriers, spark plug insulators, microwave and X-ray tube components, and thermocouple protection tubes [35]. The largest application or ceramic electrical insulators is for substrates and packages for silicon chips for integrated circuits.

Some ceramics are also used in semiconductor devices. Semiconductor materials have resistivity between that of conductors and insulators. The energy gap of insulators is so large, however, the energy gap of a semiconductor may be overcome by supplying a sufficient amount of energy which allows the electrons bridge the energy gap and conduction occurs. There are two types of semiconductors:

1.Intrinsic semiconductors

2.Extrinsic semiconductors

Intrinsic semiconductors are pure materials and semiconductivity is their inherent, natural property. Some of the group IVA materials such as Si, Ge, Sn possess intrinsic semiconductivity. Nevertheless, some intrinsic semiconductors do not have low enough resistivity to be useful at room temperature in an electronic circuit. The desired level of resistivity is achieved by introducing impurities. These impurities enhance the properties of semiconductors. These types of semiconductors are called extrinsic semiconductors and divided into two groups: n-type extrinsic semiconductors and p-type extrinsic semiconductors [25, 35].

Electronic ceramics are applied to semiconductor devices generally in the form of thin film. Films can be grown by epitaxial techniques, chemical vapor deposition, and other deposition techniques. Among the applications of ceramics in semiconductor devices are photoconductor, thermistor, photomultiplier, rectifiers, transistors, and varistors [35].

Superconductivity was first discovered in 1911 by Heike Kamerlingh Onnes. He has found that electrical resistivity was zero at 4.2 ^{0}K. This behaviour is called as superconductivity. Many substances were found that they exhibit superconductivity below a certain temperature (T_c) which is called critical temperature and materials showing this behaviour are called as superconductors. In recent years, high T_C superconductors (T_C is typically above 30^{0}K) were synthesized such as Hg-Ba-Ca-Cu-O (T_C is around 130 ^{0}K) or Bi-Sr-Ca-Cu-O (T_C is around 120 ^{0}K) compounds.

Superconducting ceramics find uses in either thin film or bulk forms in the applications of those including laboratory magnets and high energy physics. Future applications of these superconductors may contain quantum interference devices (SQUIDs), electrical power transport, magnets, motors, and in communication and computer equipment.

Dielectric ceramics, which are very important and widely used in modern technology, are another class of electronic ceramics. Dielectric ceramics can be used in the either bulk, thick or thin film form. Among the most important dielectric ceramics are PLZT (lead lanthanum zirconate titanate), PZT (lead zirconate titanate), PMN (lead magnesium niobate), $BaTiO_3$, $SrTiO_3$, etc.

Polarizability is an important property especially for dielectric ceramics. When an electric field is applied to a dielectric ceramic, the negative and positive charges are displaced at the opposite sides of the material. As a result of this displacement an electric dipole moment is created.

There are several types of polarization mechanisms such as electrical, orientation (dipolar), ionic, and interfacial polarization. Electrical polarization is observed in all dielectric materials. The mechanism is based on the very slight shift of the electron cloud around the nucleus through the positive electrode. The nucleus of atom moves in opposite direction.

Dielectric constant (relative permittivity) may be defined as the degree of polarizability or charge storage capability of a material. When an electric field is applied to the two parallel metal plate in the vacuum, one plate is

positively and the other is negatively charged. When a dielectric material is placed between these two plates, the material polarized and the density of the charges on the plates changes. The ratio of charges on the plate without a dielectric material to the charges with a dielectric material gives the relative permittivity. Dielectric constant is temperature and frequency dependent [25,35].

Dielectric breakdown strength is the maximum electric field value that a material can withstand without broken down and allowing the current to pass. When the voltage difference reach to a critical value, the current passes through the material and causes a short between the electrodes.

Ferroelectric materials involve permanently polarized crystals even in the absence of electric field. The crystal possesses a finite polarization vector due to the separation of negative and positive charges. The direction of polarization can be changed by applying the electric field.

Ferroelectric behaviour is dependent on the crystal structure. The crystal must be noncentric and must contain alternate atom positions or molecular orientations to permit the reversal of the dipole and the retention of the polarization after the voltage is removed. $BaTiO_3$ is an adequate example to ferroelectric materials. $BaTiO_3$ has an cubic structure above 120^0C (The Curie Temperature). Ti^{4+} ion lies in the center of the cube of which the oxygen ions are placed on the faces and Ba^{2+} ions are on the corners. When the crystal is introduced to an electric field, the center Ti^{4+} ion is displaced in the electric field direction and the crystal is polarized. However, after the removal of electric field, the ion reverts to its original position [25, 35].

One important parameter for the ferroelectric materials is the Curie temperature at which the ferroelectric properties of a material change. Below the Curie temperature, the structure of crystal becomes tetragonal. The center atom shifts very slightly from the center position. The center of mass of negative charges does not coincide with the center of mass of positive ions. Hence, a small dipole moment is created. However, above Curie temperature,

the structure becomes cubic, the centers coincide at the center of the cube, thus no ferroelectricity, no polarization and no hysteresis loop, and the crystal becomes paraelectric.

When the $SrTiO_3$ is cooled below the Curie temperature, the structure of a crystal becomes tetragonal, the center atom changes the position, and the crystal is polarized. During this process, not all Ti^{4+} ions shift in the same direction. Each Ti^{4+} ion has an equal probability of moving towards six oxygen ions lying on the faces of the cube. As a result, all dipoles are in the same direction. A region of the crystal in which the dipoles are aligned in a common direction is called a domain.

The direction of the polarization may be altered by applying an electric field in the opposite direction of the polarity of the original dipole. In this case, Ti^{4+} ion moves through the center of the cube and is placed at the opposite side of the original position.

Piezoelectric materials are polarized, when a stress is applied. One side of the material is negatively charged and the other side is positively charged. This effect is called as piezoelectricity. Reversible process is also available. When electric field is applied to piezoelectric material, a small amount of mechanical deformation is observed. The direction of mechanical deformation depends on the direction of the applied field.

Piezoelectricity is observed only in certain crystals. All ferroelectric crystals are piezoelectric but not all piezoelectric crystals are ferroelectric. Piezoelectricity is the property of crystals, which have no center of symmetry. 32 types of crystal classes are reported. Among these 32 types of crystal classes, 20 can exhibit piezoelectricity. These 20 types of crystal class have no center of symmetry. All types of cubic crystals have a center of symmetry. If an imaginary line passing through the center of the crystal intersects any two points on the opposite faces at a equal distance from the center, that crystal is said to have a center of symmetry. The crystal with a center of symmetry

exhibits no polarization when stressed. Because, the center of the mass of the negative charges always coincides with that of positive charges.

Pyroelectric crystals are special class of piezoelectric crystals. 10 types of piezoelectric crystal classes are pyroelectric. Pyroelectric crystals are polarized when they are heated. Heating of the crystal results in mechanical deformation due to the thermal expansion which causes a displacement in the position center atom higher dipole moment [35].

Piezoelectric ceramics generally find applications in the conversion of mechanical force to the electrical signal or vice versa. One example is the phonograph pickup. The stylus caused to vibrate by the contours in the groove of the record. The vibration is converted to an electrical signal by a piezoelectric ceramic. The electrical signal then amplified and converted into audible sound waves. Another application areas of piezoelectric ceramics are microphones, headphones, hydrophone, piezoactuators, ultrasonic cleaners, sonic devices and band pass filters [35, 38].

$LiTaO_3$ is one of the important pyroelectric materials. Pyroelectric materials have wide ranges of application areas. For example, $LiTaO_3$ is used in a scanning microcalorimeter capable of sensitivity in the submicrocalorie range. Other applications for pyroelectric ceramics include optical sensors, thermal bolometers for inferred measurements, and devices for gas-flow measurements [35, 38].

CHAPTER III

STRONTIUM TITANATE, PROPERTIES AND APPLICATIONS

Strontium titanate ($SrTiO_3$) is a ferroelectric material and has a cubic perovskite structure. In the cubic structure of $SrTiO_3$, as seen in the figure 3.1, Strontium atoms are placed at the corner of the cube and the Ti^{+4} cation is surrounded by six O^{2-} anions in a tetragonal arrangement in the cubic unit cell of $SrTiO_3$.

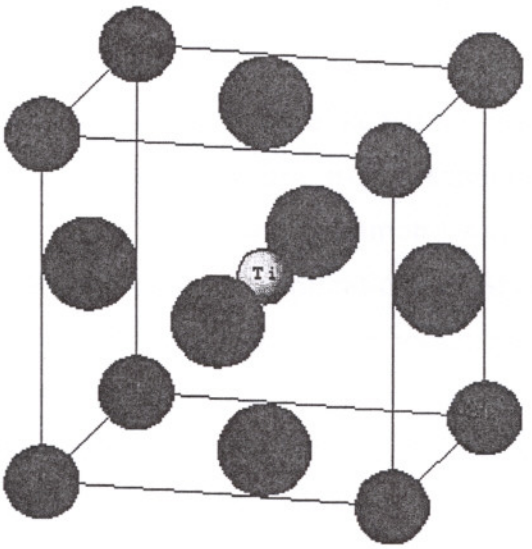

Figure 3.1. Structure of Strontium Titanate above Tc.

Perovskite ferroelectrics are of interest for high temperature and electronic applications because of its unique properties. $SrTiO_3$ possesses beneficial characteristics as a perovskite material. It has high dielectric constant, high breakdown strength, chemical and thermal stability. It has a dielectric constant of 285-320 at room temperature. The tetragonal to cubic phase transformation of $SrTiO_3$ (T_C) is 105 ^{0}K. The lattice parameters, a and c, are 3.906 Å and 3.949 Å for tetragonal structure and lattice parameter a is 3.905 Å for cubic structure [16]. Figure 3.2 exhibits the pictorial view of the tetragonal and cubic crystal structures of $SrTiO_3$. The physical properties of $SrTiO_3$ are listed in table 3.1.

Table 3.1. Physical Properties of $SrTiO_3$ [16]

Density:	5.12 g/cm^3
Melting Point:	2080 ^0C
Thermal Expansion Coefficient:	9 * 10-6 $^0K^{-1}$
Thermal conductivity:	120 milliwatts/cm °C at 100°C
Specific resistivity:	>109 Wcm

The unique properties of $SrTiO_3$ made it to find many applications in the electronic industry in recent years. Among these applications are cell capacitors in DRAMs, Internal Boundary Layer (IBL) capacitors, grain boundary barrier (GBBL) capacitors, low voltage non-ohmic thermistors (varistors), voltage controlled microwave dielectrics, electrodes for the photoassisted electrolysis of water, oxygen sensors, and as a substrate for high-T_c superconductors. $SrTiO_3$ may be readily converted into n-type semiconductor by either reduction or doping. $SrTiO_3$ is also used in the immobilization of high-level radioactive waste in ceramic form. All these applications of $SrTiO_3$, especially those based on electrical properties, depend greatly on variations in the type and amount of impurities, particle size, homogeneity and handling procedure [13]. $SrTiO_3$ is used in applications in the form of either thin film or powder.

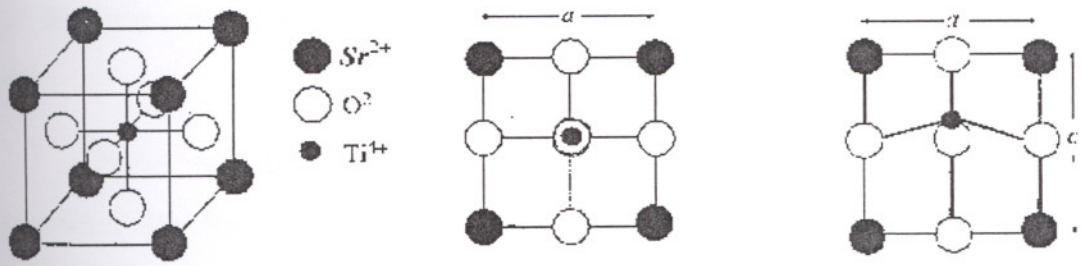

Figure 3.2. Cubic and Tetragonal Structures and lattice parameters of $SrTiO_3$

CHAPTER IV

STABLE COLLOIDAL DISPERSION PREPARATION

In ceramic processing, the stability of colloidal ceramic dispersions is very important for numerous operations such as powder preparation, milling, shape forming (slip casting, tape casting), coating, deposition, etc. The state of dispersion significantly influences the green density of sintered ceramics. The high density and homogeneity of green microstructure of ceramic compacts may be obtained by well dispersed, stable ceramic dispersions. Ceramic dispersions in liquids are commonly unstable and inhomogeneous because of the tendency of ceramic particles to agglomerate [26].

The behavior of the particles within the suspension is controlled by the mutual relation between the particles. The attraction and repulsion forces between the particles play a common role in the stability of suspension. Between two particles in the suspension, Van der Waals forces cause attraction and the similarly charged double layer around particles causes repulsion. Van der Waals forces always present, however, repulsive forces are the consequence of the interaction between particles that have similar surface charges [26, 29, 44].

There are mainly two types of stabilization method according to repulsion mechanisms between the particles, electrostatic stabilization and electrosteric stabilization. Electrostatic repulsion is based on the interaction between two identical particles, having similar surface charges, with electrical double layers. Steric repulsion is the result of the interaction between two particles with a polymers, long chained micromolecules adsorbed at the surfaces [29,44].

4.1 ELECTROSTATIC STABILITY

The stability of suspension in a polar fluid, such as water, is attained by regulating the electrostatic repulsion forces between the particles. The particles

in a liquid have a tendency to agglomerate. Agglomeration of particles is prevented by balancing the repulsive and attractive forces between the particles. The origin of the repulsive force for the suspension in the polar media is electrical double layer. Electrical double layer formed around the particle plays an important role in the colloidal stability.

4.1.1 Electrical Double layer

The behaviour and the state of the particle/liquid interface are described by the Electrical Double Layer theory. A surface electrical charge appears when a particle is introduced to a liquid. This may be as a consequence of several mechanism such as ionization, ion adsorption or ion dissolution. Surface charges of the particle attract the nearby ions of opposite charge in the surrounding solution and repel the ions of similar charge. This causes a layer around the particle of which surface charges are balanced by counter ions. As seen in the figure 4.1, Electrical Double Layer consists of two parts: inner part (also called Stern layer) which is very near to the particle surface and the outer part. In the inner part, the dimensions of ions and the short-range interactions between the ions determine the charge and potential distribution. Outer (diffuse) part consists of ions, which are in thermal motion and distributed according to the balance of electrostatic forces. In the inner part the concentration of ions are very high compared with outer part. As moving far from the particle surface, the ion concentration decays and, at last, attains the concentration of bulk solution. As the chemical equilibrium is established, the potential is balanced by the electrical charge created by the ions distributed in bulk solution and approximates to zero where as the potential at the particle surface has its maximum value [29, 44]. The distribution of potential along the path from the particle surface through the bulk solution is given by the Poisson-Boltzmann equation with Debye-Huckel approximation:

$$\psi(x) = \psi_0 e^{-\kappa x} \qquad (4\text{-}1)$$

where ψ is the potential at a distance x and κ is the inverse Debye length. κ is given by;

$$\kappa = \sqrt{\frac{2z^2e^2C_0}{kT\varepsilon\varepsilon_0}} \qquad (4\text{-}2)$$

where z is the valency, e electron charge (1.60219×10^{-19} C), C_0 is the bulk concentration of ions, k Boltzmann constant (1.38066×10^{-23} J/K), T temperature, ε and ε_0 the permittivity of the solution and vacuum, respectively. $1/\kappa$ gives the double layer thickness.

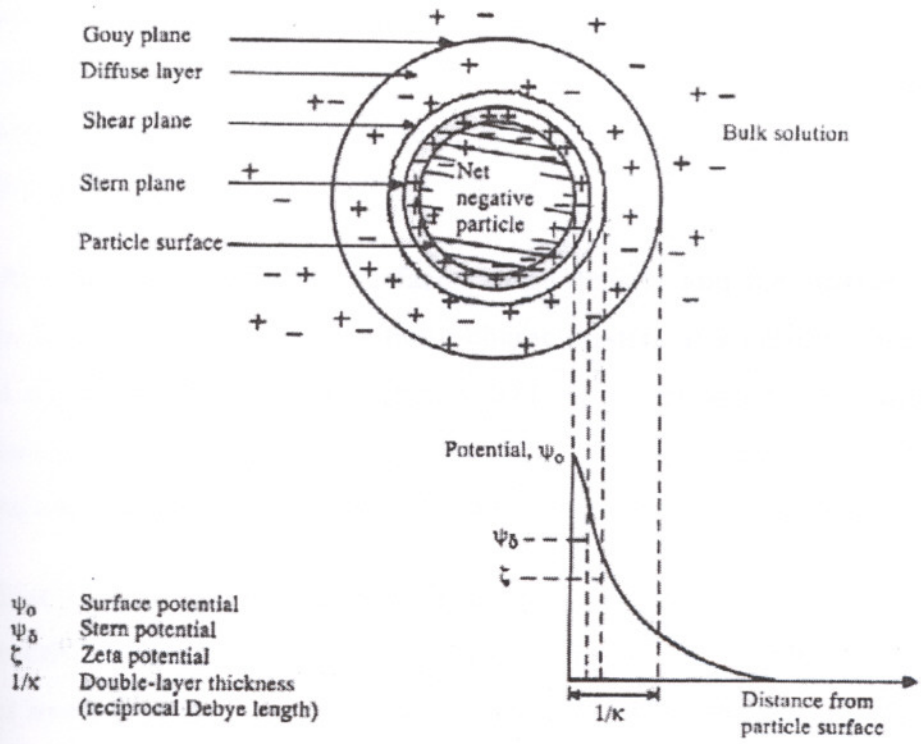

Figure 4.1. Schematic of Electrical Double Layer [44].

4.1.2 Zeta Potential

The interaction between the particles within the suspension is regulated by the overlap of their diffuse layers. Thus, the potential at the Stern layer and the diffuse double layer directly influences the interaction between the particles. With the movement of the particle surface, the ions, in a certain distance from the surface of the particles, of the approximate amount of surface charges remain with the surface. The plane at that distance is called shear plane. The

shear plane is placed slightly further away from the Stern layer. The potential at the shear plane is called zeta potential (ζ) which is slightly less than that of the Stern layer [26, 29, 44].

Zeta potential is dependent on several parameters such as pH value, permittivity of liquid, type and concentration of particles and electrolytes in the suspension. Zeta potential is very important parameter in colloidal stability and normally decays from positive values to negative values as the pH of the suspension increases. The pH value where zeta potential of a certain material is zero is the isoelectric point, pH_{iep}. It is reported that the stability of the colloid is obtained where the absolute value of zeta potential is higher than that of the isoelectric point [29].

At isoelectric point, the surface charge density and the surface potential are zero. The solid, which shows these characteristics at a certain point, is said to be at its point of zero charge (PZC). PZC is a very important parameter in determining the colloidal stability. At PZC, the dispersion is destabilized. Stabilization is achieved when the pH is kept sufficiently far from the PZC [29].

Stability of colloids is determined by the balance between the repulsive and attractive forces between the particles. The electrical double layers of two particles overlap if they are close enough to each other. The degree of electrical double layer overlap determines the rate of repulsive force between two particles if the stability is caused by the particle charge (electrostatic stabilization). The attractive force between two particles is a result of Van der Waals interaction. The interaction between two particles and the stability of powder dispersion in a polar media is described by DLVO theory. The total energy between the two particles in a suspension is given by the summation of repulsive (V_R) and attractive (V_A) forces.

$$V_T = V_R + V_A \tag{4-3}$$

The attractive and the repulsive forces are as given below:

$$V_R = 2\pi\varepsilon\varepsilon_0 a\zeta^2 \exp(-\kappa h) \tag{4-4}$$

$$V_A = \frac{-A_{12}a}{12h} \qquad (4\text{-}5)$$

where;

ε and ε_0 the permittivity of the solution and vacuum respectively, a radius of the particles, ζ zeta potential, κ inverse Debye length, h the distance between the particles, A_{12} effective Hamaker constant for the suspension.

Figure 4.2 represents change in repulsive and attractive forces and the consequent total energy curve with respect to the distance between particles schematically. Primary minimum refers to very strong aggregation at very close distances of separation where Born repulsion may occur as a result of overlap of electron clouds in the atoms. Aggregation of the particles in the primary minimum is an irreversible process. The particles in the primary minimum should exceed a potential barrier to flocculate. Very high energy is required to deflocculate the particles again. However, the flocculation of particles in the secondary minimum is a reversible process. Particles may be separated by giving a small amount of energy such as gentle stirring.

Electrostatic repulsion is controlled by changing the ionic strength, composition and the pH of the system.

4.2 ELECTROSTERIC STABILITY

In non-polar organic systems, electrostatic repulsion becomes weak and stability is achieved by steric repulsion, which is based on the interaction between long-chained polymer molecules adsorbed to the surface of the particle. These molecules may consist of hydrocarbons with acid or basic head groups or of amphipatic block copolymers. Adsorbed polymer molecules form a thick layer around the particle. This steric layer consists of loops, tails and trains as seen in the figure 4.3. The thickness of the layer depends on the concentration of polymer in the suspension, its molecular mass, the solubility of the polymer in the dispersing medium and the attractive forces between the polymer segments and the surface.

There are mainly two steric repulsion mechanisms which lead to the colloidal stability, osmotic effect and entropic or volume restriction. As two particles approach each other, the polymer layer around the particles interpenetrate which leads to an overall increase in the density of polymer segments. Therefore, osmotic pressure between the particles increases. This results in the increase in repulsive forces. Furthermore, depending on the additional approach of these two particles, the volume between the particles is limited. The volume restriction between the particles leads to an unfavourable decrease in the chain entropy, thus an increase in the overall free energy thus in repulsion [29, 44].

Unlike electrostatically stabilized suspensions, most steric dispersions are extremely sensitive to temperature variations, flocculating on either cooling or heating, This effect is reversible and can be attributed to the special polymer solvency [29].

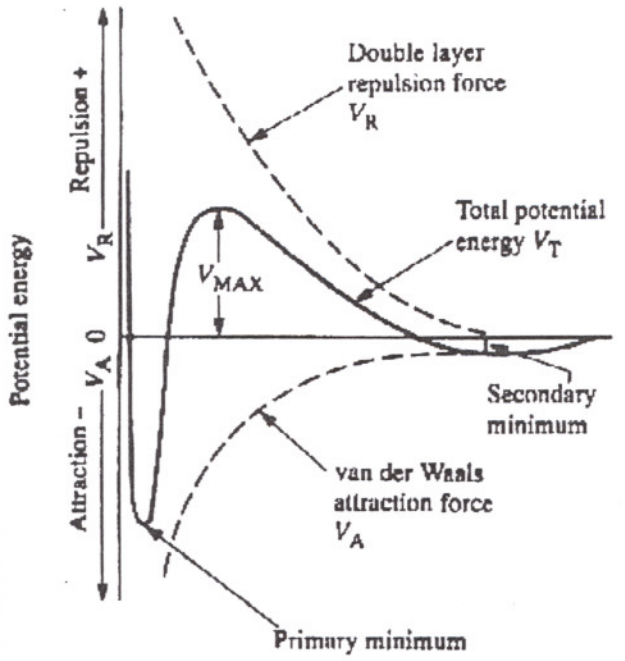

Figure 4.2. Particle-particle potential energy of interaction as a function of surface to surface separation distance [44].

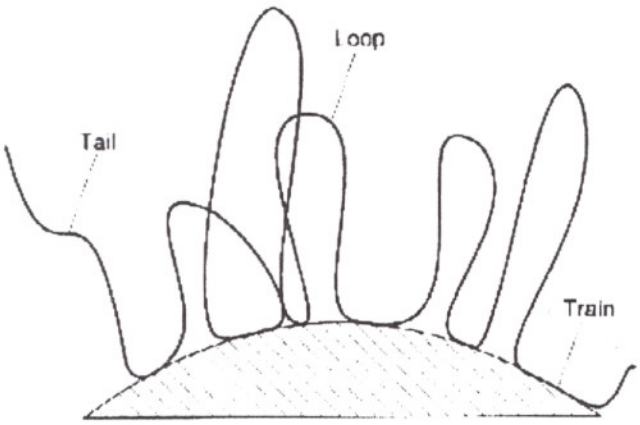

Figure 4.3. The loops, trains and tails of the molecule adsorbed onto particle surface [29].

CHAPTER V

RHEOLOGY

Rheology studies the deformation of the materials under applied stress and defines flow properties such as viscosity shear rate, shear stress, etc. The term rheology was derived from the old Greek word "Rhe" which means flow. When liquids are subjected to stress, they deform reversibly or irreversibly. The response of a liquid against the applied stress is generally expressed as viscosity. The viscosity of a fluid is a measure of the internal resistance offered to the relative motion of different part of fluid.

Fluids are basically divided into two classes according to the behaviour indicated against applied shear stress, Newtonian, and non-Newtonian fluids. Figure 5-1 is known as the flow curve or rheological diagram and shows the relation between shear rate and shear stress. Newtonian fluids possess a linear proportionality between the shear rate and shear stress. In this case, when a force is applied to the fluid of a given surface area, the fluid immediately begins to flow. As the force per area is increased, the velocity of flow increases proportionally. In rheology, the force per unit area is called shear stress and the velocity of flow is rate of shear. Mathematically, the relationship is expressed as follows:

$$F/A=\tau = \eta(dv/dy) \qquad (5.1)$$

where:

$F/A=\tau$ = shear stress

dv/dy= velocity gradient (shear rate)

η= Proportionality constant (viscosity)

Some examples to Newtonian fluids are water, alcohol, glycerin, syrup, etc.

Non-Newtonian fluids are classified into three groups, plastic pseudoplastic and dilatant fluids. Plastic fluids, also called as Bingham materials, exhibit similar behaviour with Newtonian fluids but the difference is that plastic fluids do not flow until a certain value of shear stress is reached. The point where fluid begins to flow is called as yield point and the magnitude of shear stress at this point is called as yield stress. The behaviour of these liquids is expressed by Bingham model:

$$\tau - \tau_y = \mu\gamma \qquad (5.2)$$

where:

τ_y = yield stress

γ = shear rate

This type of flow behavior is typically observed in suspensions and other viscous liquids like ketchup.

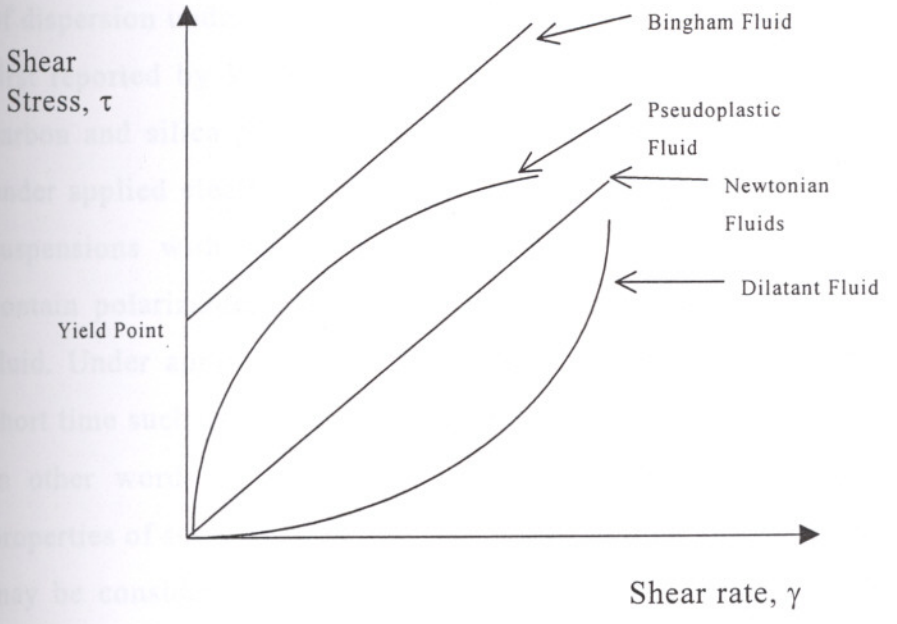

Figure 5.1. Rheological diagram.

The second type of non-Newtonian flow behavior, pseudoplastic fluid is non-linear. The flow begins immediately when the stress is applied, however, the viscosity of the liquid decreases with increasing shear stress. In other words, increasing shear rates results in a gradual increasing of shear stress. This type of flow behavior is also called shear thinning. The examples are toothpaste, whipped cream or weakly flocculated suspensions.

As in the case of pseudoplastic flow, in dilatant systems the flow begins immediately when the stress is applied. As the stress is continually applied, however, the viscosity of the liquid increases. These types of liquids (eg., suspensions with a solid content of more than 50%) are called shear thickening.

There are two other types of fluids, thixotropic, rheopectic fluids, which are the subclass of pseudoplastic and dilatant fluids, respectively. The viscosity of thixotropic fluids decreases as time goes by whereas rheopectic fluids exhibit an increase in viscosity with time.

5.1 Electrorheology

Electrorheology may be defined as the change in rheological properties of dispersion under applied electrical field. Electrorheological phenomenon was first reported by W. M. Winslow in 1949. His studies were including starch, carbon and silica particles in oil [1]. He observed the fibrillation of particles under applied electric field and subsequent change in rheological properties of suspensions with respect to applied electric field. Electrorheological fluids contain polarizable, dielectric particles dispersed in low-dielectric, insulating fluid. Under applied electric field, particles form fibrils and chains in a very short time such as milliseconds and suspension exhibits resistance against flow; in other words its apparent viscosity increases. Change in the rheological properties of suspension is observed under applied electric field. The suspension may be considered as solidified. However, following the removal of electric field, the suspension reverts to its original state. Electrorheology is not only in the interest of academics but also in industry, because its unique properties

make it possible to transfer energy and control motion efficiently [20]. ER fluids are investigated for the uses in some applications such as in some automobile parts (brakes, clutches), valves, robotic controls, etc. However, some technical problems appear in the usage of ER fluids such as long term suspension stability, temperature range, and high power demand for heavy-duty applications.

Electrorheological fluids are composed of polarizable particles dispersed in insulating oil. The dimensions of the particles are reported in the range of 0.04-100 μm in diameter [2, 15, 20, 48]. It is reported that although neither the lower nor the upper limit of the particle size was strictly defined, the upper size of the particles should be one-tenth of the electrode spacing. The lower limit is also due to fact that at some level, Brownian motion may dominate interactions that give rise to the ER effect [2, 20]. Many ER fluid compositions were investigated. The particles were chosen from both organic and inorganic materials. Among these materials are zeolites, ion exchange resins, starch, flour, strontium titanate, titanium dioxide, silica, glass, etc. These particles were dispersed in oils having high dielectric breakdown strength and low electrical conductivity. The oil may be cooking oil, silicon oil, mineral oil and halogenated hydrocarbons. Some ER compositions are listed and investigated in details in [2, 15].

Many particle-oil variations were studied by many researchers. The properties of particle and oil properties are important to optimize the ER effect. Some researchers listed properties of both particles and oils. The particles should have high dielectric constant, and electrical breakdown strength, low conductivity. Density of particles influences the sedimentation rate. Particles with a high density generally have more tendency to settle down. Oils should have low conductivity, high electrical breakdown strength and low viscosity.

The particle concentration in the ER fluid has a great influence on the ER effect. The concentration is generally chosen between 0.05 and 0.50. ER fluids

at very low particle concentrations do not exhibit strong and significant ER effect. At high particle concentrations, it is observed that fluid may conduct electricity at high electric field, which causes a drop in ER effect. The zero field viscosity may be very high at high concentration, which is not preferable.

Electrorheological fluids generally exhibit Newtonian behavior prior to the application of electric field. However, following the application of electrical field the fluid approximates to Bingham model [1, 15, 22, 43]. The rheological behaviour of the Bingham fluid is described by.

$$\tau(\gamma, E) = \tau_0 + \mu\gamma \qquad (5.3)$$

τ=Shear Stress, τ_0=Field dependent yield stress, γ=shear rate, μ=viscosity

Upon application of electric field, the particles are polarized. As a result of polarization, the attraction and repulsion forces appear between the polarized particles and result in subsequent chain and fibre formation. As a result of these chain and fibre formation, ER fluid shows certain strength against flow. The flow of fluid is set as the deformation of these chains begins. The yield stress is a very critical parameter for the suitability of electrorheological fluids in applications, especially in stress transfer applications. Below the yield stress, the electrorheological fluids show solid like behaviour. On applying an electric field to the electrorheological fluid, a significant increase in the amount of yield stress is observed, while the plastic viscosity is not changed inherently [22].

The main phenomenon of the ER effect is polarization. Two polarization types are considered. One is extrinsic polarization and the other is intrinsic polarization. Extrinsically polarisable ER fluids include hydrophilic particles that require water or some other polar activator (low molecular weight alcohols or amines) to obtain measurable ER activity. The amount of water required to optimize ER effect is 1-10%. Water consistency limits the temperature range for ER applications. High temperatures cause water to evaporate and subsequent decrease in ER effect. High voltages applied to ER fluid cause heating.

Extrinsically polarisable particles are categorised as polar non-ionic and polar ionic materials. The formers are polar hydrophilic solids that contain only a trace amount of mobile ions (e.g. polysaccharides), the inorganic oxides with surface hydroxyl group (e.g. silica or alumina). Polar non-ionic materials generally exhibit little ER effect when an activator is not present. Because there are few mobile ions to form dipoles by charge separation and because the materials generally have low permittivities, one hypothesis is that polarization results from alignment of the dipoles of the high permittivity polar activator sorbed on the surface of the particle [20].

In contrast, polar ionic materials contain mobile ions. These materials are generally polymeric salts that allow large dipoles to be formed by charge separation of ions. In most cases, a polar activator is needed to provide ion solvation and mobility. Monovalent ions usually provide the best performance possibly because they are easily solvated and are very mobile.. The monovalent salts of polymeric carboxylic acid may be given as an example.

Intrinsically polarisable materials do not require polar activator. That is why the temperature range for ER activity is expanded. Intrinsically polarisable materials can function predominantly by bulk polymerisation (e.g. ferroelectrics and liq. Crystals) or by interfacial polarization (e.g. metals, semiconductors and insulated conductors). Ferroelectrics can develop large dipole moments by the alignment of existing molecular dipoles or by the field induced distortion of crystal structures. The polarization can be obtained without flow of ions or electrons across the particle, so the polarization does not contribute to overall conductivity. Because the polarization is the result of molecular dipoles [20].

Conducting and semi-conducting materials develop large dipoles by allowing electrons or protons to flow along extended delocalised conductance bands. Conducting and semi-conducting materials develop large dipoles by allowing electrons or protons to flow along extended delocalised conductance

bands. Conducting and semi-conducting materials are polarized very fast and create very large dipoles.

In case of contact between conductive particles after imposition of electric field, the loss of dipole is observed as a result of particle to particle charge transfer. This causes considerable reduction in ER effect.

To supply the ER effect, ac or dc field is used. DC field causes electrophoresis (collection of particles onto one electron). To prevent electrophoresis pulsed DC or AC field is used. ER fluids are frequency dependent. At high frequencies, particles might not be polarized on time. Particle should reverse its polarization fast enough. For any ER system, there will be an AC frequency over which ER effect will drop. At very high frequencies no ER effect is detected. Pulsed DC decreases the electrophoresis mobility, improves on AC by increasing ER stress and decreasing the power consumption. Pulsed DC offers the flexibility to modify ER properties by changing the pulse frequency and length.

There are many possible applications of electrorheological fluids. The possible applications of electrorheological fluids are mostly based on the ability of force transfer of these fluids and vibration damping [20]. Possible devices include electrorheological clutches, brakes, hydraulic valves, active damper systems, and robotic control systems.

CHAPTER VI

POWDER PROCESSING OF ELECTRONIC CERAMICS

In recent years, advanced ceramics such as electronic ceramics found many application areas with developing technology. Various types of electronic ceramics are formulated by using different techniques. These techniques affect the properties and morphology of the ceramics. For any application, ceramic material should have convenient properties. To obtain desired properties, the preparation method should be selected precisely. Conventional methods such as mixed-oxide and precipitation methods have been used for many years to synthesise ceramic powders. However, some disadvantages and limitations come with the conventional methods. In recent years, chemical methods are developed to prevail desired properties of ceramics.

Chemical methods allow to control the properties of electronic ceramic powders. Sol-gel and Pechini (liquid-mix) methods are included in the chemical preparation methods. For electronic ceramics, electrical properties such as dielectric constant, dielectric breakdown strength are important for any specific application area. Chemical methods include such opportunities to control the state of aggregation, purity, stoichiometric ratios, and homogeneity, which have affect on the electrical properties of ceramics powders.

6.1. Mixed Oxide Method

Mixed oxide method is a very old method in the preparation of multicomponent oxide ceramic powders. It is based on the calcination of the mixture of the salts of desired cation at very high temperatures. The oxides, carbonates or hydroxides of desired cations may be used as a raw material. The purity of the raw material is one of the designation factors for the purity of ceramic powder. The salts of desired cations are well-mixed and grinded in a ball mill and calcined at very high temperatures. The solid state reactions take

place in a mixed oxide method. The homogeneity of the product may be enhanced by repeating the grinding and the firing steps.

Although the mixed oxide method is relatively cheap, there are some limitations and disadvantages. Solid state reaction does not ensure the homogeneity at the molecular level. The powder may have a wide range of particle size distribution. It is not easy to control the properties. After calcination, the product may contain some impurities which can be the result of incomplete removal of carbonates and other compounds during calcination, or can be introduced during grinding and milling steps in metallic or ceramic media. Grinding , milling and sizing steps may be required to obtain desired particle size [29, 35].

The mixing oxide method is used for the fabrication of many multicomponent oxide ceramic powders. Electronic ceramics such as dielectrics are most widely prepared powders by mixed oxide method.

6.2. Coprecipitation Method

Coprecipitation method is another conventional method, which is based on the precipitation of hydroxides or oxalates from the aqueous solution of cations. Single or multicomponent oxide ceramic powders may be prepared by this method. The aqueous solution of desired cations is prepared by solving the salts in water, hydrolysing the alkoxides in the presence of acid. At very low pHs a clear solution is obtained. By introducing this aqueous solution to high pHs, cations are precipitated. The mixture of components is obtained during precipitation. The precipitates are washed to remove the undesired ions. The precipitates are dried, milled and calcined to achieve ceramic powder [29, 35].

Coprecipitation method does not ensure the purity of the product. The powder may contain impurities. It is not easy to control the reaction parameters. The particle sizes are not homogenous and the particle size distribution may be wide.

6.3 Sol-gel method

Sol gel method is getting importance in the preparation of advanced ceramics in recent years. This method makes it possible to prepare ceramic powders with desired properties, good purity, and homogenous particle distribution. Sol-gel process involves the hydrolization of alkoxides in the presence of some additives and is a colloidal route to ceramics in which the gelation takes place after the formation of sol.

Sols are colloidal systems in which the solid particles in liquid medium, having at least one dimension in the range of 1-100 nm, are dispersed in a dispersion medium. Sols are very stable, very homogenous and may stay stable without formation of gel in several months. The stability of sol is the result of strong, long-range columbic attractions between the particles. Sols are highly concentrated dispersions, have very ordered colloidal network, and may be easily converted into gels by various methods [26, 31].

Gels, the coagulated form of sol, have polymer-like three-dimensional network of solid particles throughout the sol. In the gel structure, solid particles form a solid network and a large amount of solvent is entrapped in this network. Sols may be converted into gel form by drying (removal of the solvent entrapped in the gel structure) or addition of a suitable electrolyte. The rigidity of gels prevents the migration or segregation of atoms during drying and assures the homogeneity at the molecular level [26, 31].

The sol gel method simply involves the hydrolysis of the metal alkoxides in the presence of alcohol and acid. Since the sol-gel route to ceramic powder involves a liquid phase chemical reaction, the end-product is free to dust. The liquid phase reaction offers a ceramic powder with good purity. The powder produced has a homogenous particle distribution and large surface area, which permits lower calcination temperature. Desired properties of ceramic powder may be easily obtained by controlling the reaction parameters of sol gel process. Sol gel route allows the produce ceramic powders with specific properties.

Allowing to produce particles with specific sizes avoids crushing and grinding steps required by conventional processes. Sol-gel route also permits to develop special materials, or configurations such as films, controlled-size spherical powders, fibers, or monoliths.

The expense of alkoxide is the disadvantage of sol gel method. However, this disadvantage may be compensated by using salts of desired cations instead of alkoxides in the production of multicomponent oxide powders [26]. Another disadvantage of sol-gel process arises from the fact that cracks may appear during drying process. In addition, multi-step processing results in additional process time and cost [31].

Alkoxides are the raw materials in the preparation of ceramic powder via sol gel method. Alkoxides are molecules in which a metal atom is bounded to a alkyl group via oxygen. The general formula of metal alkoxides is given as M-(O-R)n where M is metal atom and R is alkyl group. Alkoxides are very sensitive to humidity and CO_2 in the air. Thus, they must be handled under an N2 atmosphere. Hydrolyzation of alkoxides can be carried out by the addition of water to the alkoxides. Hydrolyzation and condensation reactions are the main reactions taking place during sol gel route to ceramic powders.

$$M(O-R)_n + xH_2O \longrightarrow M-(OH)_n + xR-OH \qquad \text{Hydrolysis}$$

$$M-(OH)_n \longrightarrow M-O_{n/2} + \frac{n}{2} H_2O$$

$$M(O-R)_n + nM'-OH \longrightarrow nM-O-M' + nR-OH \qquad \text{Condensation}$$

Since alkoxides are not miscible with water, the sol gel reaction takes place in the presence of a common solvent, such as an alcohol. Especially, the parent alcohol of the alkoxides is used as a solvent, otherwise, an alcohol exchange reaction may take place [1]. A homogenous mixture at molecular level

is obtained by solving the alkoxides in alcohol. The solvent selection is very important to solve the alkoxides completely.

Single component oxides may simply be prepared by hydrolyzing the alkoxide of desired cation. However, some limitations may come up with preparation of multi component oxides. In the preparation of multi component oxides, multi component alkoxides or combination of single component alkoxides may be used. However, in the latter case, some problems such as inhomogeneities may arise, since the hydrolysis rate differs from one alkoxide to another. This problem may be eliminated by using salts instead of alkoxides [26, 29, 6].

Following the mixing of all components, a clear solution should be obtained. Cloudiness or precipitation indicates a segregation of components. The water and alkoxides react to generate the structure leading to the sol-gel transition. This reaction is referred as hydrolysis of alkoxides and is performed by adding water to alkoxide-alcohol solution under vigorous stirring. The purity of water is very important, so that distilled water is used for hydrolysis.

In the sol gel method, acid is used for peptization of the solution. The type and the amount of acid are very important in the sol gel process. Usually HNO_3, Acetic acid and HCl are most widely used acids. It is reported that the type of acid plays a much more important role than the pH of the system [26]. Hydrolysis at low pH produces a gel that can be calcined to oxide whereas hydrolysis at high pH nucleates oxide powder directly from solution [29].

Most metal alkoxides are very reactive towards hydrolysis and condensation. They must be stabilized to avoid precipitation. The chemical control of these reactions is currently performed by adding complexing reagents that react with metal alkoxides at a molecular level, giving rise to new molecular precursors of different structure, reactivity, and functionality. The amount of acid used for peptization influences the shape and size of the particle [26].

Gel is formed by drying or by adding suitable electrolyte, after the formation of sol. Changing the pH and destabilization of sol may lead to sudden formation of gel. Huge amount of liquid phase is entrapped in the gel structure. The liquid phase may be removed by drying the gel. The rate of drying process influences the characteristics of the gel. High drying rates may cause cracks in the gel structure, while very low drying rates may allow to obtain bulk shapes [6].

In fine powder preparation, many drying methods are used such as freeze-drying, spray drying and air-drying. The agglomeration is an important problem during drying and the strongest agglomerations are especially observed in the air-dried powders. However, freeze-drying method yields powders with less aggregation [26].

6.4. Pechini Method

The Pechini (liquid mix) method is a polymeric route to oxide ceramics. It is a chemical process for ceramic powder synthesis, which was originally developed by Pechini during 1960s. The main route of the Pechini method is to obtain a perfect mixture of metal cations at the molecular level. Complex compositions may be prepared by Pechini method, which permits to produce over 100 different oxide compounds including high-temperature ceramic superconductors such as $La_{1.85}Sr_{0.15}CuO_{4-\sigma}$ and $Yba_2Cu_3O_{7-\sigma}$[29]. Some examples to oxide ceramic powders prepared by Pechini method are listed in Table 6.1.

Pechini method has advantages compared to conventional powder processes. Pechini method allows controlling the stoichiometry, which results in preparing advanced ceramic powders of desired properties. In addition, resin may be converted into oxide at low temperatures. For example, the temperature of 1273 K where $BaTiO_3$ powder is produced by solid state reaction between $BaCO_3$ and TiO_2 is reduced to 923 K by using Pechini method [29]. In other chemical processes, such as in sol-gel or coprecipitation methods, high-level

cation segregation may occur during precipitation, hydrolysis or condensation. However, it is believed that less segregation of various cations would occur during the charring step since the cations are entrapped in the char. Moreover, the mixing of cations at the molecular level ensures the high purity of the end-product [27].

Table 6.1 . Powders made by Pechini Method [29].

Titanates:	$BaTiO_3$, $SrTiO_3$, $Pb(La,Zr,Ti)O_3$
Niobates:	$BaNb_2O_6$, $Pb_3MgNb_2O_9$
Zirconates:	$CaZrO_3$
Chromites:	$LaZrO_3$, $MgCr_2O_4$
Ferrites:	$LiFeO_2$, $CoFe_2O_4$
Manganites:	$LaMnO_3$, $YMnO_3$
Aluminates:	$LaAlO_3$, $MgAl_2O_4$
Cobaltites	$LaCoO_3$, $YCoO_3$
Silicates:	Zn_2SiO_4

In Pechini method, simply the metal atom is bounded by a polycarboxylic acid, heating results in polyesterification and further heating causes polymeric resin. An aqueous solution of desired metal cations are prepared in alpha-carboxylic acid (for example citric acid, poly-acrylic acid, and mucic acid). Perfect mixing of metal cations at the molecular level may be obtained by preparing aqueous solution of metal cations in the presence of acid and polyhydroxy alcohol (such as ethylene glycol). Chelate complexes of metal cations with polycarboxylic acid undergo esterification reaction when heated with the alcohol at around 80^0 to 110 ^{0}C. Figure 7.1 shows the chelation and polyesterification reactions taking place in Pechini process. Further heating at moderate temperatures (around 150-250 ^{0}C) induces a black ash, which yields powder when calcined at high temperatures. Calcination temperature is generally between 400-600^0C. Subsequently, final product is obtained by oxidizing the cations at 500 to 900^0C.

Pechini method is a quiet complex process and there are many parameters affecting the final product. The ratio of water:acid:alcohol will affect the final product. Moreover, the heating schedule during gel setting, charring and calcination affect the final agglomerate morphology.

Using poly(acrylic acid) (PAA) adds some benefits with regard to lead to a cross-linked polymer resin, which may provide more homogenous mixing of the cations and less tendency for segregation during charring and calcination. The functionality of poly(acrylic acid), 28, is higher than that of citric acid, 4. Thus, the higher functionality of PAA should greatly aid in the formation of a cross-linked resin [27].

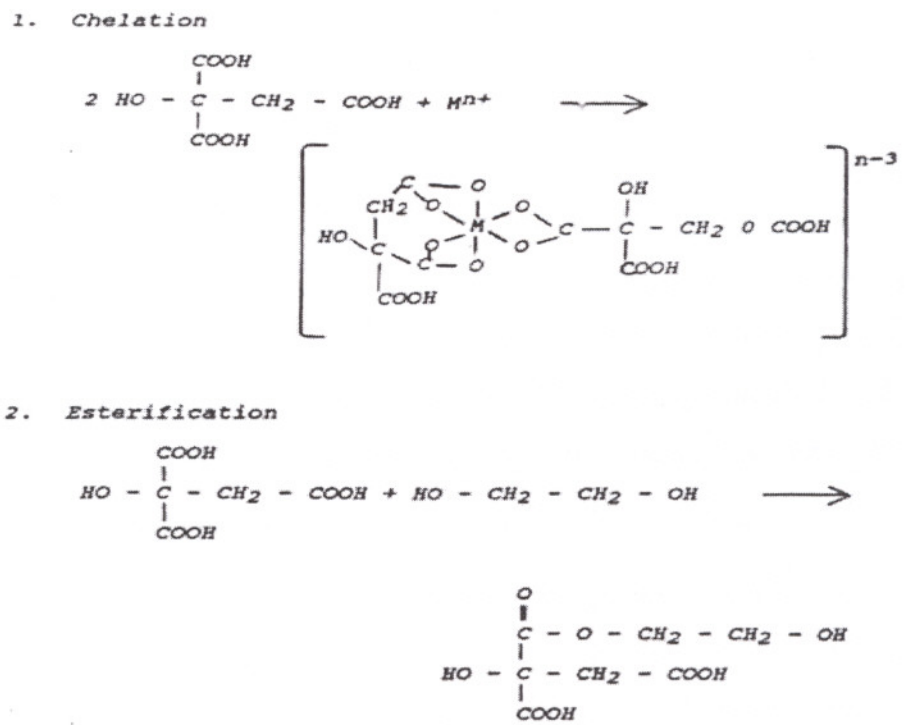

Figure 6.1. Chelation and Polyesterification reactions.

CHAPTER VII

EXPERIMENTAL WORK

7.1 Chemicals and Materials

Titanium alkoxide was purchased from Aldrich, with minimum purities of 97.5% for titanium (IV) isopropoxide. Strontium nitrate ($Sr(NO_3)_2$) and ethylene glycol (EG) were purchased from Aldrich with purities of 99+% and 99.8%, respectively. Poly acrylic acid (PAA) at molecular weight of 2000 was also purchased from Aldrich. 2-Propanol (2-P), and nitric acid (NA) with purities of >99.5% and 65%, respectively were purchased from Merck. Anhydrous citric acid (CA) was also purchased from Alfa.

Oils (Depar White oil, Tech-40) used in electrorheological experiments were purchased from Interyag Petroleum Products Industry and Trading Limited Inc., Izmir, Turkey.

7.2 Powder Preparation Methods

In this study, $SrTiO_3$ powders were prepared by sol-gel and Pechini methods. In sol-gel method, the strontium titanate powder preparation was based on the TiO_2 sols studied by Caglar [5]. In sol-gel method, $SrTiO_3$ powders were prepared by using titanium isopropoxide (TISP), isopropyl alcohol (2-P), nitric acid (NA), and strontium nitrate. In the Pechini route, the same procedure outlined by Peschke [32] was used.

Sol-Gel Method: In sol-gel method, two powders were prepared. The alcohol:Ti^{4+}, water:Ti^{4+} ratios and amount of chemicals are listed in Table 7.1. A required amount of TISP was mixed in half the total amount of 2-P under continuos stirring. The acidic solution was prepared in a separate beaker by mixing the remaining half of the 2-P and NA solution under constant stirring. A stoichiometric amount of $Sr(NO_3)_2$ was dissolved in distilled water in a separate

beaker. This solution was further added to the acidic solution. The flow diagram of sol-gel method is given in Figure 7.1.

Table 7.1. The chemicals and quantities used in sol-gel process.

	Ti(ISP) (ml)	Alcohol (ml)	Acid (ml)	$Sr(NO_3)_2$ (gr)	Water:Ti^{4+}	Alcohol:Ti^{4+}
TC2	5	62.8	0.6065	3.386	2	13
TC5	12.5	78.8	1.51	8.676	2	6

Pechini Method: The chemicals and quantities used for the preparation of 2 Pechini powders are given in table 7.2. In the first batch, EG and TISP were mixed in 250 ml Erlenmeyer flask and the solution was mixed by a magnetic stirrer and heated on a hot plate for 15 minutes prior to the addition of CA. A required amount of CA was added to the above solution and the solution was stirred until a clear, yellow and viscous solution was obtained. The temperature was increased gradually. The $Sr(NO_3)_2$ solution in 125 ml of distilled water was added to the above solution. The solution remained clear and heated above 100 ^0C to boil off the water. The process was complete when about 100 ml of clear yellow solution remained. The flowsheet of the Pechini process was given in the Figure 7.2.

In the batch achieved by PAA, 50% by weight of CA was substituted by PAA. The mixture was allowed to mix for 15 minutes and PAA was added slowly after the addition of the whole amount of citric acid.

Table 7.2 . The chemicals and quantities used in the Pechini Process

	EG (ml)	Ti(ISP) (ml)	CA (mg)	PAA (mg)	$Sr(NO_3)_2$ (gr)
PCA100	35.7	20.88	18.52	-	14.4147
PCA50	35.7	20.88	9.26	9.26	14.4147

7.3 Charring and Calcination of Precursor Solutions

The gels obtained from sol-gel method were dried at 100 ^{0}C in an oven (Nuve FN 500). The dried gel was calcined at 650 ^{0}C for two hours with a heating rate of 10 ^{0}C/min in a high temperature furnace (Carbolite RHF 1600).

The precursor solution obtained from Pechini method was divided into 3 beakers in equal amounts and heated on a hot plate until a viscous, bubbly mass was obtained. Glassy resins were obtained upon cooling. These resins were charred at 250 ^{0}C for 30 minutes in a box furnace (NUVE MF120). Calcination was performed in a box furnace following the charring process. The calcination conditions are given in Table 7.3 which was based on previous work by Peschke [32].

Table 7.3. Calcination schedule for Pechini Process.

	Calcination Temperatures (^{0}C)	
PCA100	550 for 1 h.	700 for 2 h.
PCA50	400 for 1h.	600 for 2 h.

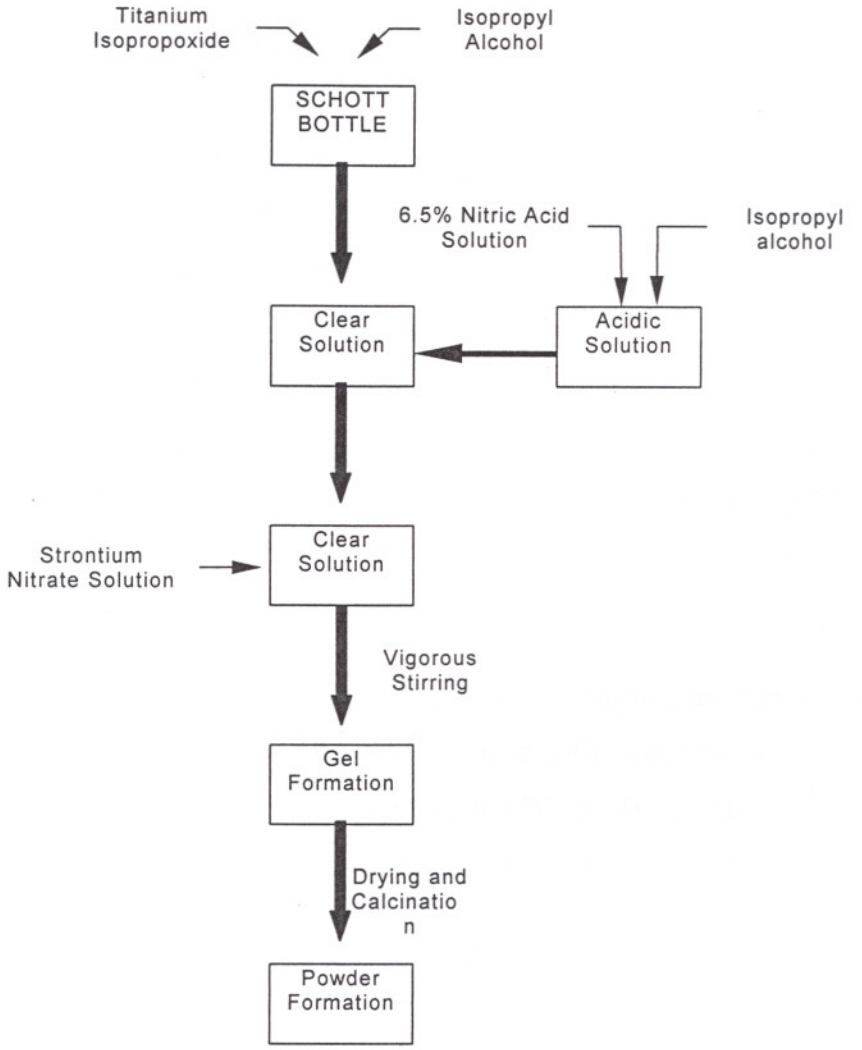

Figure 7.1. Flowsheet of sol-gel Process.

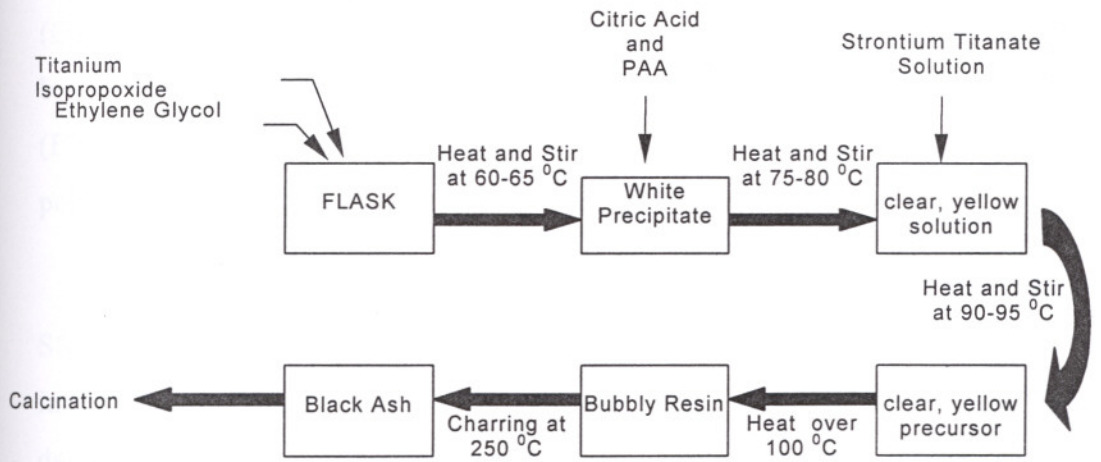

Figure 7.2. Flowsheet of the Pechini Process.

7.4 Characterization of the Powders

The characterization of powders were performed by using Fourier Transform Infrared Spectrophotometer (FTIR-8201, Shimadzu) and Thermogravimetric Analyzer (TGA-51/51H, Shimadzu) and XRD (METU, Metallurgical and Materials Engineering Department). The infrared spectra of $SrTiO_3$ samples were taken by Fourier Transform Infrared Spectrophotometer (FTIR-8201, Shimadzu) using KBr pellet techniques. A typical pellet contains 1-2 wt% sample in KBr and was prepared by mixing 0.004 gr $SrTiO_3$ powder with 0.2 gr. of KBr. The mixture was ground in a mortar and pressed under vacuum by applying 8 tonnes of pressure.

Thermal properties were examined by Thermogravimetric Analyzer (TGA-51/51H, Shimadzu). Samples of the dried gels were heated in a dry N_2 stream at a heating rate of 10 ^{0}C/min up to 1000 ^{0}C. In TGA analysis, the weight loss of 10 mg. sample as a function of temperature was determined.

SEM examinations of the powders were performed by SEM (JEOL 5200) provided by School of Dentistry, Ege University. Uniaxially pressed powders were coated with gold in order to perform the SEM observation. In order to determine the microstructure of the sintered powders an optical microscope (OLYMPUS BX-60) was used. The sintered pellets were mounted into Bakelite by mounting press (BUEHLER Simplimet 2) polished by Grinder/Polisher (BUEHLER Metaserv 2000). Prior to optical microscope analyses, the mounted pellets were chemically etched with 10% HCl solution.

Powders were uniaxially pressed at 100 MPa by a hand press (Shimadzu SSP-10A) and its attachments. Approximately 0.75 gr of powder was loaded into the die. Dimensions of the pressed pellets were measured and the green densities were determined. The pellets were sintered at 1400 ^{0}C for two hours in a high temperature furnace (Carbolite RHF 1600). The bulk densities were

determined according to Archimedes principle by using a density determination kit (Sartorius BP 210S) after sintering.

7.5 Suspension Preparation

Powders were milled in ethyl alcohol for 5 hours and ultrasonically treated for 1 hour for the breakdown of agglomerates. After ultrasonic treatment the suspension was dried at 50 ^{0}C in an oven (Nuve FN 500).

The suspensions of $SrTiO_3$ in various solids loading were prepared by dispersing $SrTiO_3$ powder in white oil. The powder-oil mixtures were prepared in a beaker by mixing with a magnetic stirrer. At very low concentrations ultrasonic treatment was also applied. However, the ultrasonic treatment was observed nave no effect on powder dispersion after a certain solids loading. The powder was slowly added into the 30 ml of oil while stirring. The weight percentages of SrTiO3 in oil were 1, 5 and 10 vol%, for PCA50 powder.

A commercial lubricant oil dispersant (Chevron Chemicals, Oloa 1200-Ashless Succinimide Dispersant) was used to disperse the powder in oil.

7.6 Rheological Experiments

The rheological behavior of $SrTiO_3$ suspensions was investigated by using a rheometer (Brookfield DV-III RV). The rheological experiments were carried out at different shear rates by using ULA adaptor of the rheometer.

A special set-up was designed and constructed for electrorheological experiments which was attached to the rheometer and a DC power supply (LABCONCO, Model 433-3290). The electrorheological experiments were performed with 10 vol% suspension. 25 ml of suspension was used in the experiment. 500 V/mm was applied to the suspension. The diagram of the set-up for electrorheological experiment is as seen in Figure 7.3.

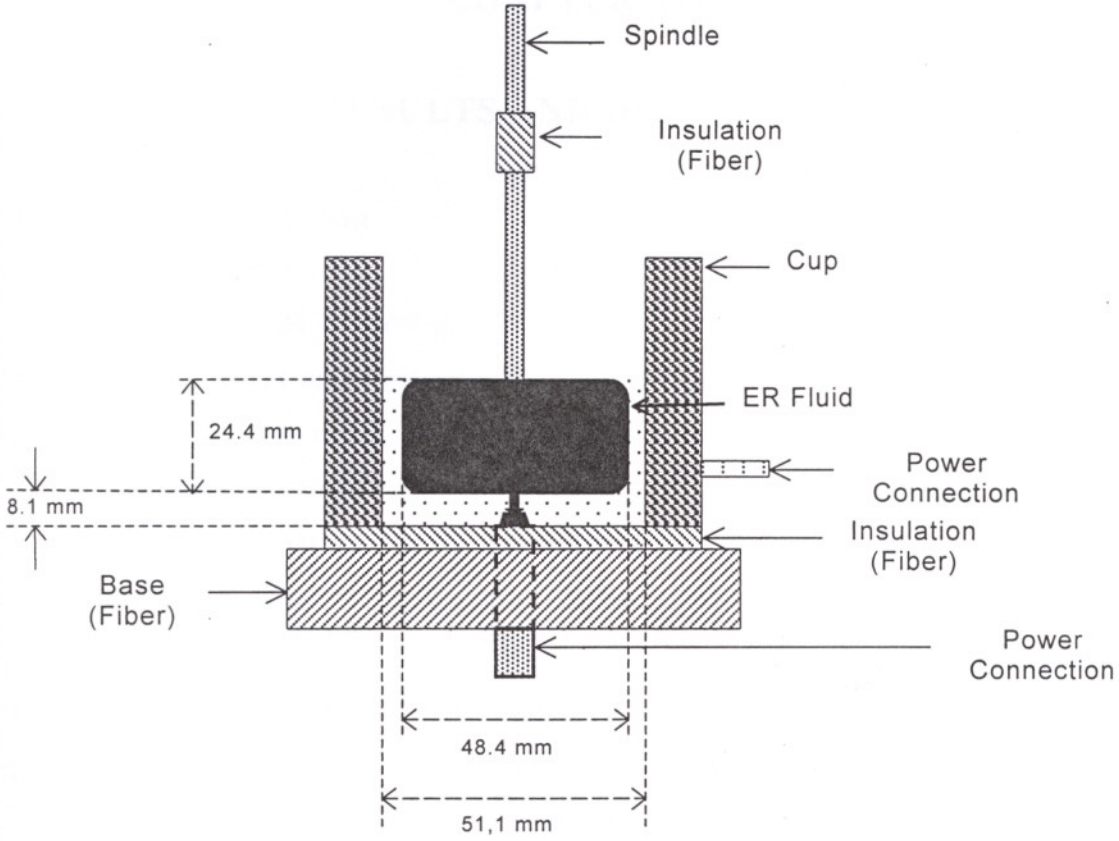

Figure 7.3. Pictorial view of the set-up designed for electrorheological experiments.

CHAPTER XIII

RESULTS AND DISCUSSION

8.1 Powder Preparation

Two methods of powder preparation were used in powder preparation section: the sol-gel and Pechini methods. Sol-gel method is based on the TiO_2 sols studied by Caglar [5]. $SrTiO_3$ powders were prepared from the gels based on TC2 and TC5 sols. During sol preparation, no precipitation was observed. Following the addition of HNO_3 solution-2-propanol mixture, the sol remained clear. However, after the addition of $Sr(NO_3)_2$ solution gelation occurred in a couple of seconds due to this reason. The addition of the $Sr(NO_3)_2$ solution was accomplished in a very short time to ensure the complete mixing of sol particles. All of the $Sr(NO_3)_2$ solution was added at once. The gelation of TC2 based gels took a longer time than that of the gels based on TC5 sols. As a result, it is possible that mixing in a smaller scale was achieved for TC2 based sols. Gels formed after the addition of $Sr(NO_3)_2$ solution were blurry and white in colour. This is most likely due to precipitation. The gelatinous mass released its liquid content partially after a short while.

Powders prepared by Pechini route was similar to the procedures reported earlier by Peschke [32]. The batches carried out by 100% CA and 50%PAA-50%CA were chosen. Following the addition of Ti(ISP) into EG, the solution became milky and viscous. The stirring and heating were performed for 15 minutes and due to the heating of the solution viscosity decreased. Heating should be carried out very carefully. The solution was kept at about 50-60 ^{0}C. After 15 minutes, CA was added gradually and completely dissolved. Temperature was in the 70-80 ^{0}C range. At higher temperatures segregation was observed at the bottom of the Erlenmeyer flask. However, at low temperatures, the solution became very viscous and difficulties in the dissolution of CA were observed. CA remained in as a bulky mass. A yellow and clear solution was obtained after the complete dissolution of CA. The addition of $Sr(NO_3)_2$ solution made no changes in appearance of the solution.

8.2 Powder Characterization

8.2.1 Thermogravimetric Analysis of Sol-Gel Precursor Solutions

In this study, only the TGA analyses of sol-gel precursors were carried out. The TGA studies of Pechini powders had been done by Steven L. Peschke [32] as discussed before. The calcination temperatures for Pechini based powders were chosen by referring to his study. TGA analyses of sol-gel powders were performed in order to decide on the optimum calcination temperature, which leads to impurity free powders.

Figure 8.1 shows plots of the weight loss and percent reduction in weight vs. temperature for the precursors of the sol-gel method. Water and organics completely disappeared at around 400 ^{0}C as seen in Figure 8.1. The large amount of solvents entrapped in the gel structure was already removed during the drying at 100 ^{0}C. The major weight loss around 550-680 ^{0}C for TC5 and around 550-650^{0}C for TC2 is due to the decomposition of nitrates. Beyond 700^{0}C, no significant weight loss was observed and this exhibits that the formation of $SrTiO_3$ may be carried out at around 650-700 ^{0}C.

TGA curves indicate that approximately 30% of initial weight loss occur in between 575 ^{0}C and 675 ^{0}C. This weight loss was due to the removal of nitrates. The weight loss in this temperature range was estimated to be more than this value, when the amount of nitrates in the starting chemicals ($Sr(NO_3)_2$) was taken into account. It was estimated that during gelation about 3/4's of the free Sr^{2+} ions were bound to nitrates again. However, 1/4 of the Sr^{2+} ions were assumed to be bound on the surface of TiO_2 nanoscale particles. The free nitrate ions were assumed to be lost before 575 ^{0}C. This result may point to a better mixing between Sr^{2+} and Ti^{4+} ions in sol-gel powders than in simple mixing of two separate solid phases.

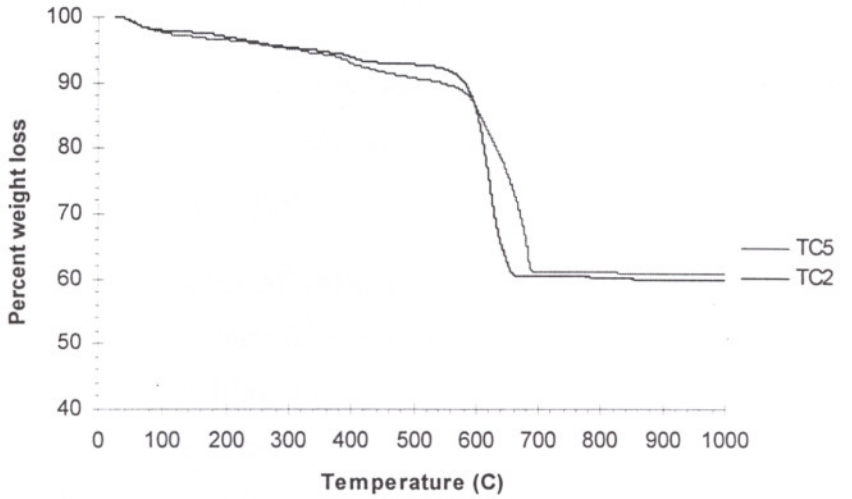

Figure 8.1. TGA curves of dried TC2 and TC5 based intermediate precursors.

8.2.2 FTIR Analyses of the powders

The FTIR analyses of the powders were performed in order to characterize the structure of precursors and to control the quality of the powders after calcination.

FTIR spectra of sol-gel derived powders before calcination is given in Figure 8.2. The sharp absorption band around 1390 cm^{-1} may be assigned to asymmetric stretching absorption of the NO_3 group of the nitrate salt. During drying, the large amount of solvent entrapped in the gel structure was removed. However, at low temperatures nitrates are still present. The two peaks between 730 and 830 cm^{-1} may be also due to the absorption band of the nitrate salt. The broad band around 3440 cm^{-1} may be due to absorption of N-H bond. The region between 500 and 700 cm^{-1} is generally assigned to inorganic titanates, M-O stretch. The broad peak at 2450 cm^{-1} possibly indicates the presence of NH bond. The absorption around 1450 cm^{-1} may indicate the presence of $-CH_2$ and $-CH_3$ groups. The assymetric NH_3^+ deformation absorbs at 1640 cm^{-1}.

As it can be seen in Figure 8.3, the peaks at 3440, 2450, 1640, 1390, 830 and 730 cm^{-1} disappeared and two new peaks around 550 and 400 cm^{-1} appeared. The intensities of these peaks increased and these peaks became more evident after calcination. The absorption bands of the certain bonds in this region may interact and the intensities of the peaks may decrease resulting in the formation of such a noisy spectrum. The peaks observed in this region may belong to M-O, N-O or N-H bonds and $-CH_2$, $-CH_3$ groups. However, the formation of $SrTiO_3$ phase and the removal of other substances during the calcination may lead to the observation of more distinct peaks belonging to M-O bonds only. The peak around 400 cm^{-1} corresponds to the titanate absorption band for titanates and the peak around 570 cm^{-1} may be assigned to Ti-O stretching mode for $SrTiO_3$.

Figure 8.4 shows the FTIR spectra of the resin charred at 250^0C for 30 minutes. The intense peaks at 1405 and 1550 cm^{-1} may be due to the typical antisymmetrical and symmetrical stretching vibrations for carboxylate ions, which are due to breaks in polyester chains and formation of ionic bonds

between the metal ions and the carboxylate groups. Esters give an absorption band in the 2750-2950 cm^{-1} region, which may be assigned to -CH, $-CH_2$ and $-CH_3$ carbon-hydrogen stretching vibrations. Cho et al. [7] reported that esters formed as a result of esterification of carboxylic acids with ethylene glycol were still present at 450 ^0C. The absorption band at 2920 cm^{-1} may be due to carbon -hydrogen stretching vibrations of esters. The broad band at 3440 cm^{-1} may be attributed to N-H bond. The intense peak at 440 cm^{-1} corresponds to the formation TiO_2 at the charring temperature. This peak showed that charred precursor contained TiO_2 phase.

As it can be seen from Figure 8.5, the spectrum of the Pechini powders indicated the same behaviour with that of the sol-gel powders. The typical $SrTiO_3$ absorption bands were in the region of 560-600 cm^{-1}. The titanate absorption bands for the $SrTiO_3$ powders were observed around 400 cm^{-1}. These results were very compatible with the results reported in the literature [7, 8, 37].

As seen in the Figures 8.3 and 8.5, there is a remarkable difference in the intensity of the peaks in the region of 400-700 cm^{-1}. The intensity of the peaks at around 400 cm^{-1} for sol gel powders is higher than that for Pechini powders. The intensity of these peaks is also higher when compared with the peaks around 600 cm^{-1} which are most likely assigned to Ti-O stretching band for $SrTiO_3$. The broad and very weak band in the region of 3300-3600 cm^{-1} is probably due to adsorption band for TiO_2. This may point to the presence of TiO_2 phase which also explains the higher intensity of 400 cm^{-1} peaks than the peaks at 600 cm^{-1}. These observations along with the XRD patterns may indicate that the formation of $SrTiO_3$ was not complete and impurity phases such as TiO_2 are present in the powders. The spectrum of Pechini powders agrees with the XRD results. No peak was observed in the region of 3300-3600 cm^{-1}. The presence of SrO phase may lead to the more intense peak at around 600 cm^{-1} for PCA50 powder.

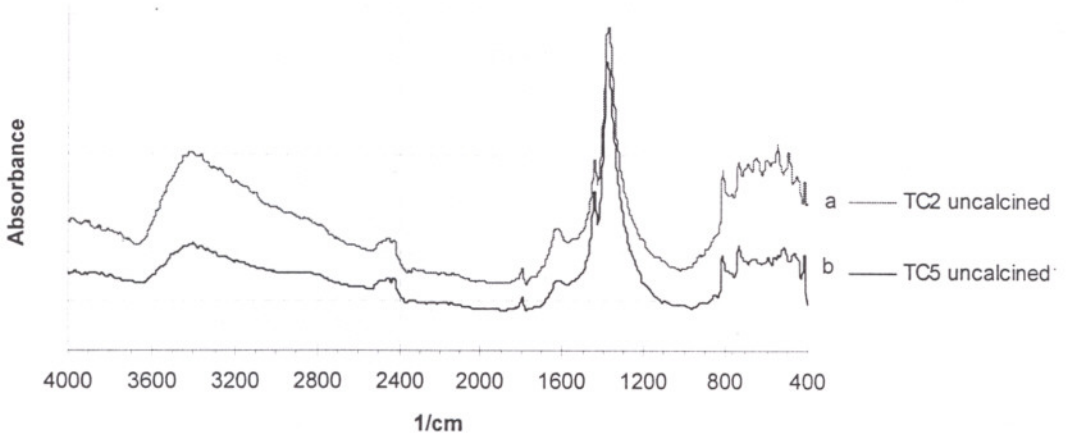

Figure 8.2. FTIR spectrum of (a) TC2 and (b) TC5 precursors before calcination.

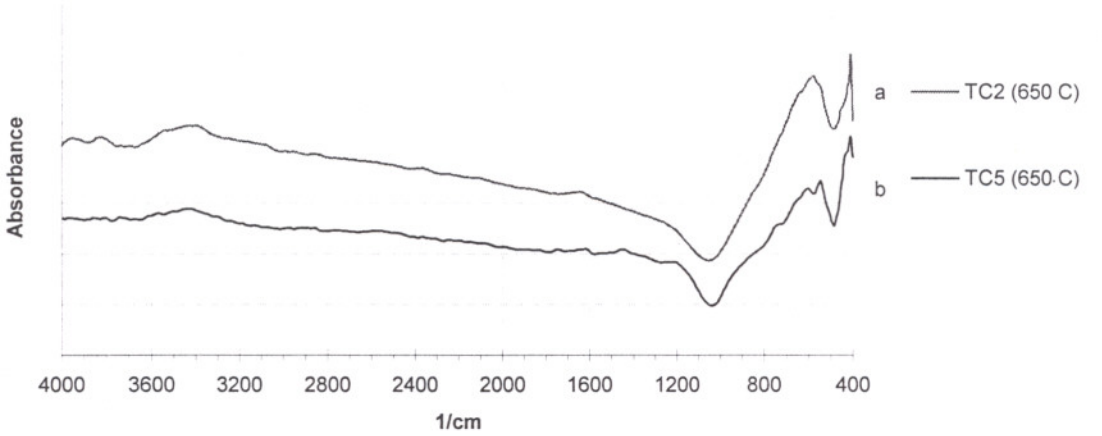

Figure 8.3. FTIR Spectrum of a) TC2 and b) TC5 derived $SrTiO_3$ powders.

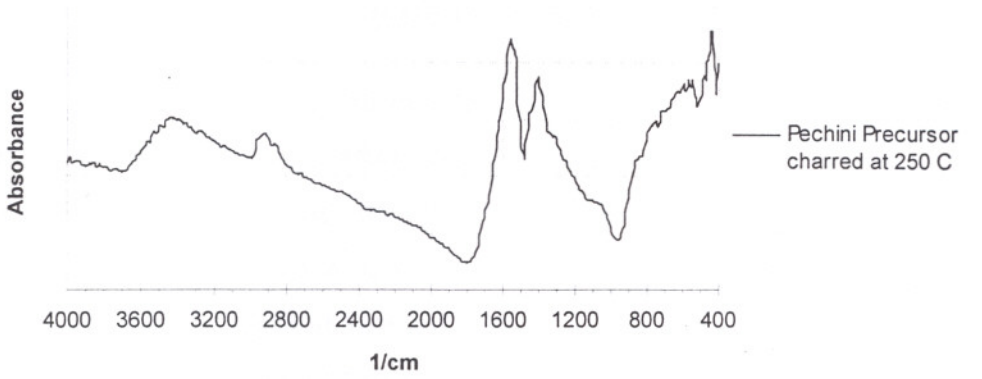

Figure 8.4. FTIR spectra of PCA50 resin precursor charred at 250 ^{0}C.

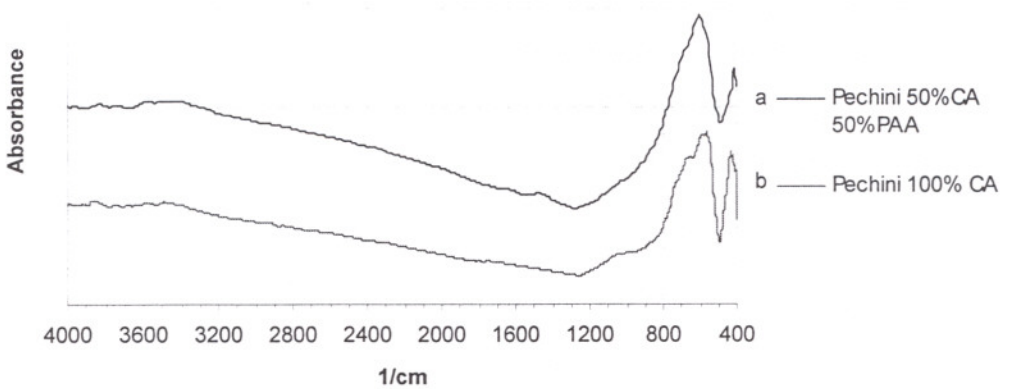

Figure 8.5. FTIR spectrum of a) PCA50 and b)PCA100 powders.

8.2.3 XRD Analyses of the Powders

X-ray analyses of the powders were performed in order to determine the nature of phases formed after calcination. Figure 8.6 through 8.8 show the X-ray diffraction patterns of PCA50, PCA100 and TC2 derived powders, respectively. In Figure 8.6, the XRD pattern of $SrTiO_3$ powder prepared by modified Pechini method was indicated. As seen from the figure, typical peaks of $SrTiO_3$ phase were observed. No more peaks except those of $SrTiO_3$ were detected. However, the XRD pattern of PCA50 powder includes a new phase identified by computer matching. The low intensity peak at 2θ values of 25 matches to SrO phase. In the study done by Steven L. Peschke [32], two additional phases were observed in the XRD pattern of similar powder calcined at different temperatures. These phases were SrO and $SrCO_3$. It was discussed that decomposition of $Sr(NO_3)_2$ produces SrO and the reaction between SrO and CO_2 forms $SrCO_3$. However, in the present work only SrO was detected as an impurity phase in the XRD pattern. The XRD pattern of the PCA100 powder were in good agreement with the results of the study performed by Cho et al. [8] and Peschke [32].

The XRD pattern of TC2 derived $SrTiO_3$ powder had many impurity phase peaks besides those of $SrTiO_3$ peaks (Figure 8.8). 14 phases including $SrTiO_3$ phase were identified by computer matching. These phases were TiO_2 phase and 12 other phases involving different molecular formulas of Ti-O and Sr-O compositions.

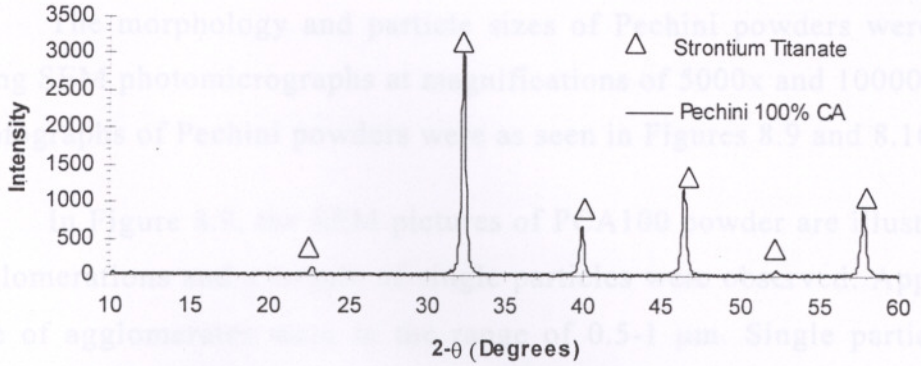

Figure 8.6. XRD pattern of PCA100 powder .

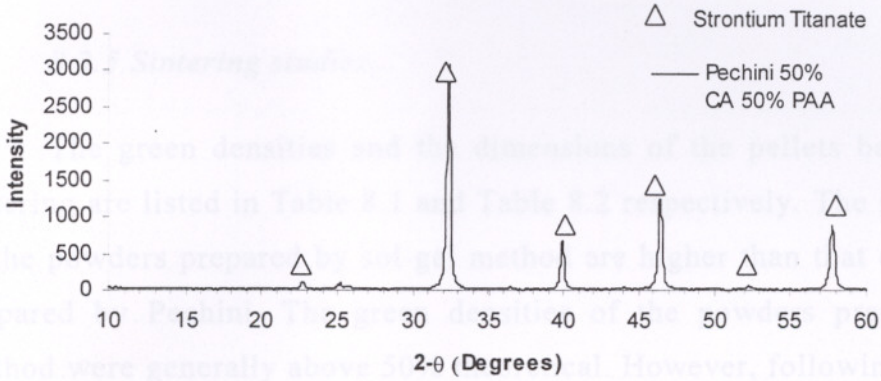

Figure 8.7. XRD Pattern of PCA50 powder.

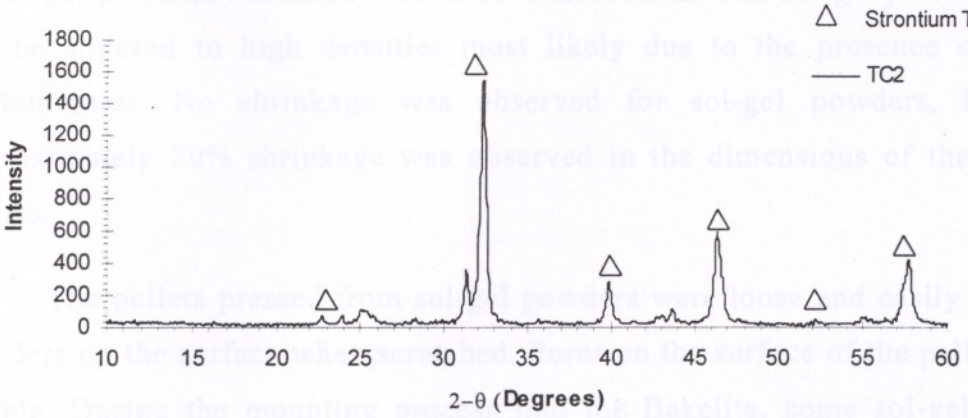

Figure 8.8. XRD Pattern of TC2 powder.

8.2.4 SEM analysis

The morphology and particle sizes of Pechini powders were performed using SEM photomicrographs at magnifications of 5000x and 10000x. The SEM photographs of Pechini powders were as seen in Figures 8.9 and 8.10.

In Figure 8.9, the SEM pictures of PCA100 powder are illustrated. Some agglomerations and a couple of single particles were observed. Apparently, the size of agglomerates were in the range of 0.5-1 μm. Single particles may be considered as approximately spherical and the sizes ranged between 0.2-0.3 μm. Figure 8.10 also exhibited the similar results. The average agglomerate size vary between 0.5-1 μm and average particle diameter size was in the range of 0.2-0.5 μm. This results matched with that of Steven L. Peschke [32].

8.2.5 Sintering studies

The green densities and the dimensions of the pellets before and after sintering are listed in Table 8.1 and Table 8.2 respectively. The green densities of the powders prepared by sol-gel method are higher than that of the powders prepared by Pechini. The green densities of the powders prepared by each method were generally above 50% theoretical. However, following the sintering process the bulk densities of the Pechini powders exhibit much higher theoretical densities than that of the sol gel powders. The bulk densities of Pechini powders were typically well above 90% theoretical while the densities of sol-gel powders remained around 60% theoretical. The sol-gel powders could not be sintered to high densities most likely due to the presence of strong agglomerates. No shrinkage was observed for sol-gel powders, however, approximately 20% shrinkage was observed in the dimensions of the Pechini pellets.

The pellets pressed from sol-gel powders were loose and easily gave off powders on the surface when scratched. Pores on the surface of the pellets were visible. During the mounting process into the Bakelite, some sol-gel powder pellets were easily cracked and an important part of the powders were lost from the surface. This was the result of very strong agglomerates resulting in very

low compaction. However, Pechini powders did not show such that behaviour. The surfaces of the Pechini powder pellets were very smooth, and the compaction was significantly better.

Table 8.1 . % theoretical densities of powders before and after sintering

Powders	Calcination Temperatures (^{0}C)	% Theoretical Density (Green Bodies)	% Theoretical Density (1400 ^{0}C)	Open Pore %
PCA100	550^{0}C/700^{0}C	49.4	92.7	0.39
PCA50	400^{0}C/600^{0}C	48.2	95	0.41
TC2	650 ^{0}C	57.3	58	12.90
TC5	650 ^{0}C	59.7	62	10.16

Table 8.2. Dimensions of the pellets before and after sintering.

Powders	Calcination Temperatures (^{0}C)	Dimensions before sintering		Dimensions after sintering (1400 ^{0}C)	
		D (cm)	t (cm)	D (cm)	t (cm)
PCA100	550^{0}C/700^{0}C	13.05	2.25	10.47	1.80
PCA50	400^{0}C/600^{0}C	13.09	2.48	10.65	2.03
TC2	650 ^{0}C	13.06	1.95	12.96	1.94
TC5	650 ^{0}C	13.07	1.80	12.95	1.80

Figures 8.11 through 8.13 show the optical microscope pictures of sintered pellets at different magnifications. Each pellet was chemically etched with 10% HCl solution. Figures 8.11 a and b illustrate the photomicrographs of TC2 and TC5 based $SrTiO_3$ powder pellets at a magnification of 1500, respectively. As seen from the Figure 8.11a, there were wide cracks and pores on the surface of the pellet. The cracks and pores were mostly as a result of applied high pressure during the molding process. The grain sizes were not distributed uniformly. This may be due to strong agglomerates or variations in particle sizes. The grain sizes were in the range of 3-5 μm.

The pellets pressed from TC5 based $SrTiO_3$ powders showed similar results. These cracks and pores on the surface mostly formed during the molding process. However, the apparent number of cracks and pores were less

than that on the surface of TC2 pellets. Nonuniform distribution of grain sizes was observed. The sizes of the grains varied between 2-5 μm.

The surfaces of the Pechini powder pellets were relatively crack-free in comparison with the surface of sol-gel powder surface. The grains were more evident and had larger dimensions. The apparent grains in Figure 8.12 were in the range of 2-10 μm in sizes. No porosity was observed at the grain boundaries.

It is evident that the grain sizes of PCA100 powders were larger than that of the PCA50. The grain sizes of PCA50 were around 2-4 μm and PCA50 had relatively more uniform grain size distributions.

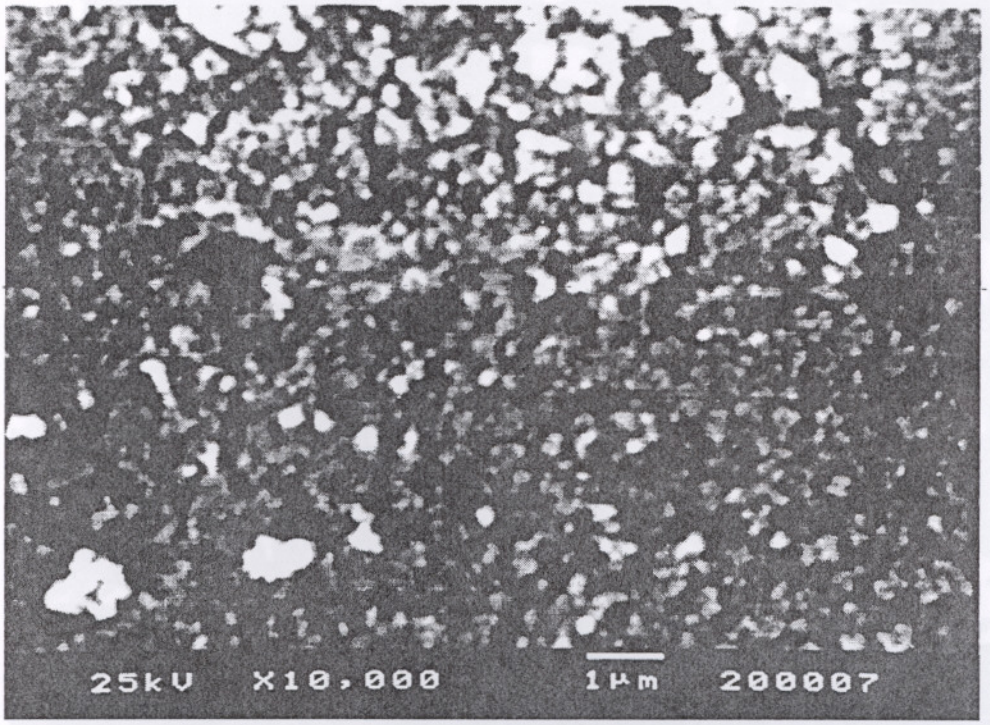

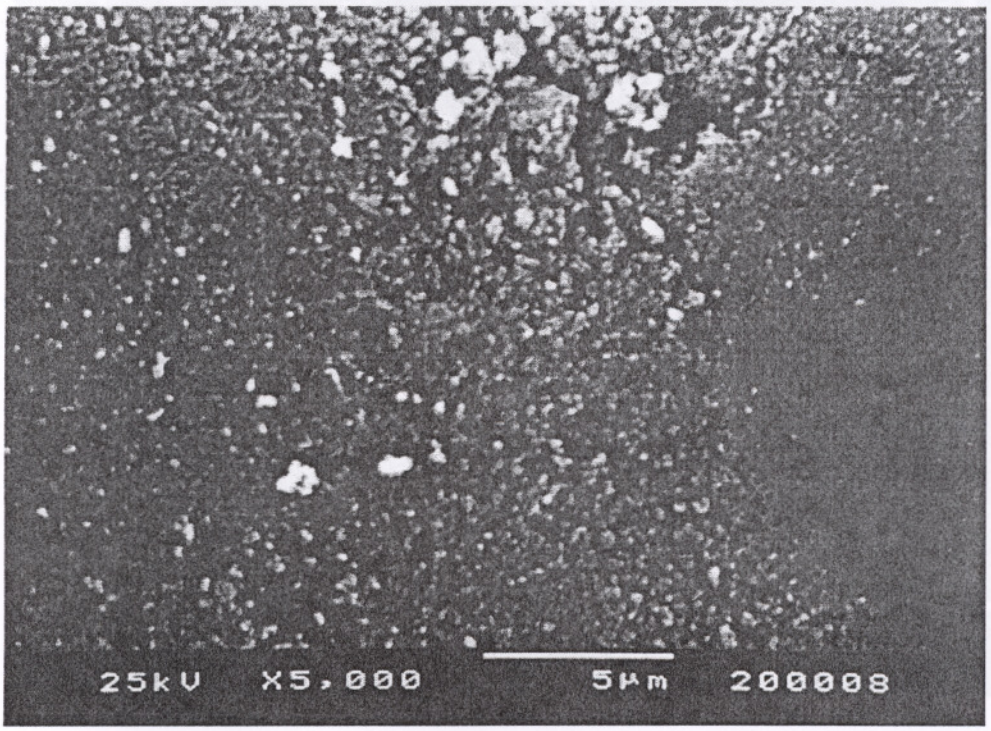

Figure 8.9. SEM micrographs of PCA100 powder at magnifications of x10k and x 5k.

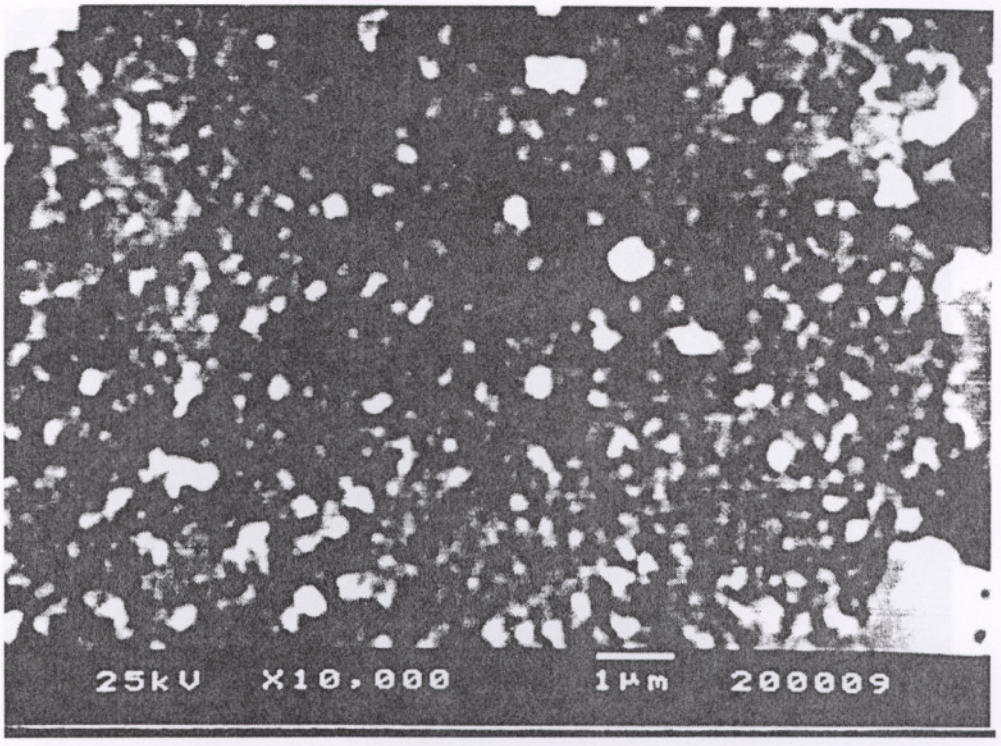

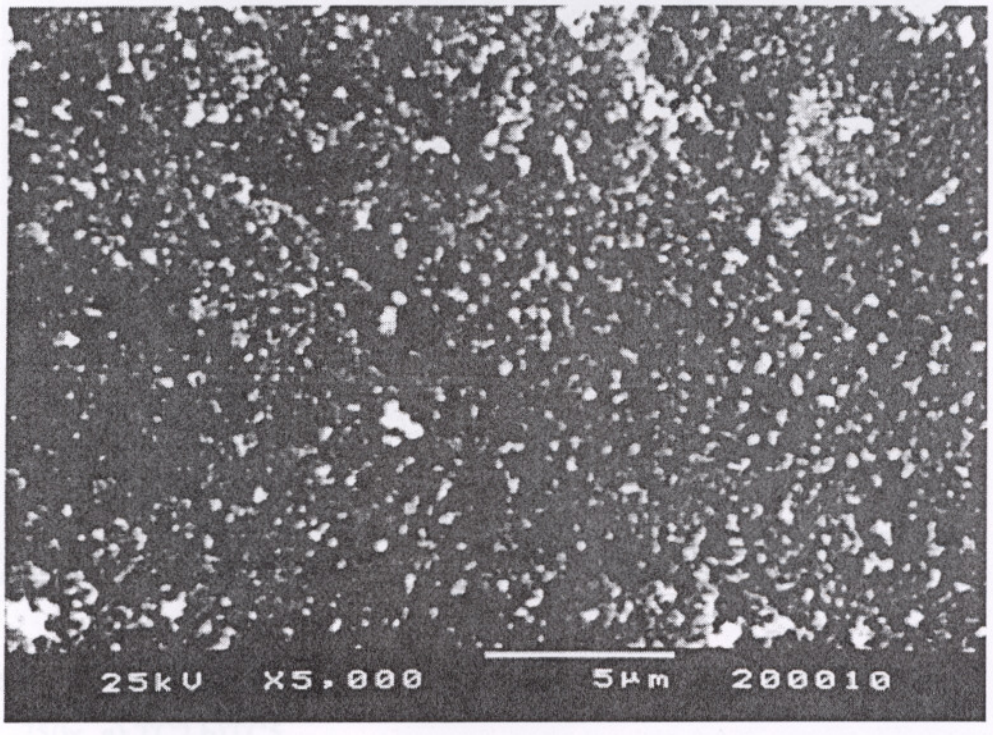

Figure 8.10. SEM micrographs of PCA50 powders at magnifications of 10k and 5k.

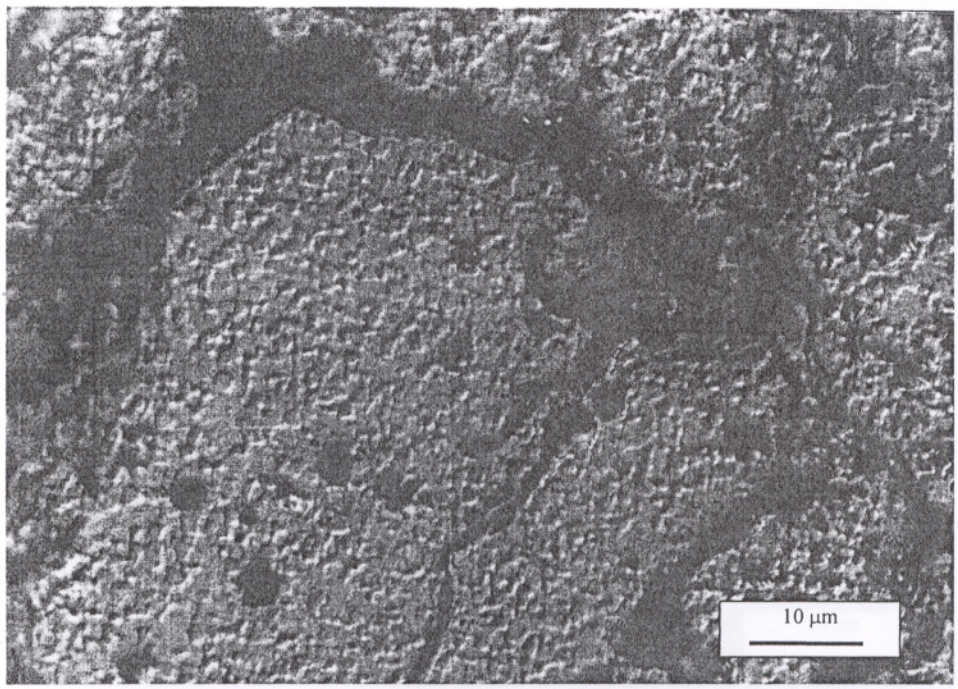

(a)

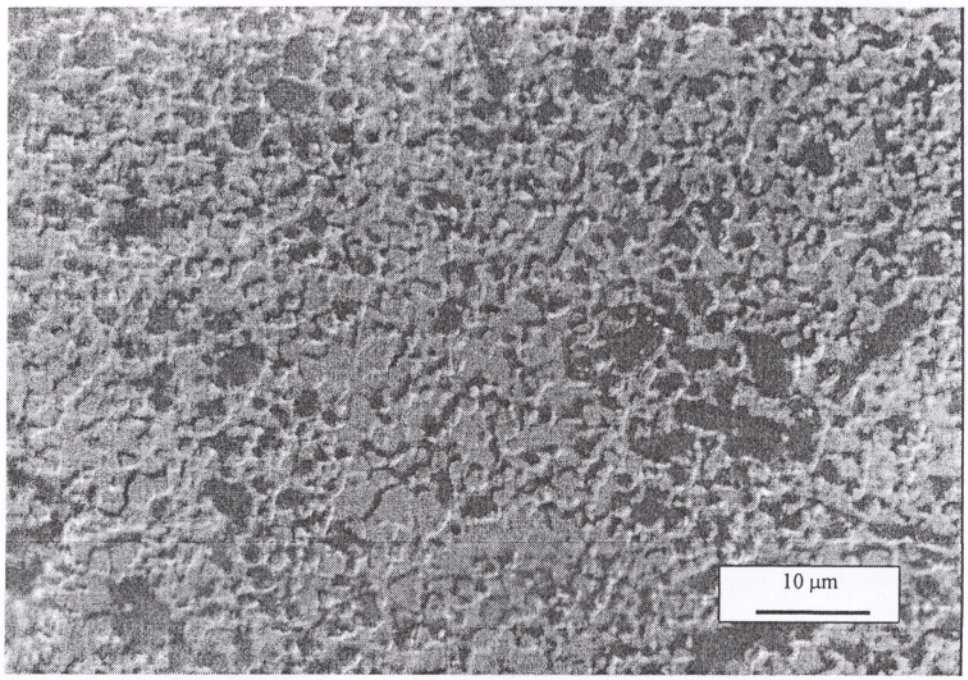

(b)

Figure 8.11. The photomicrographs of sol-gel powders at a magnification of 750x, a) TC2 b)TC5.

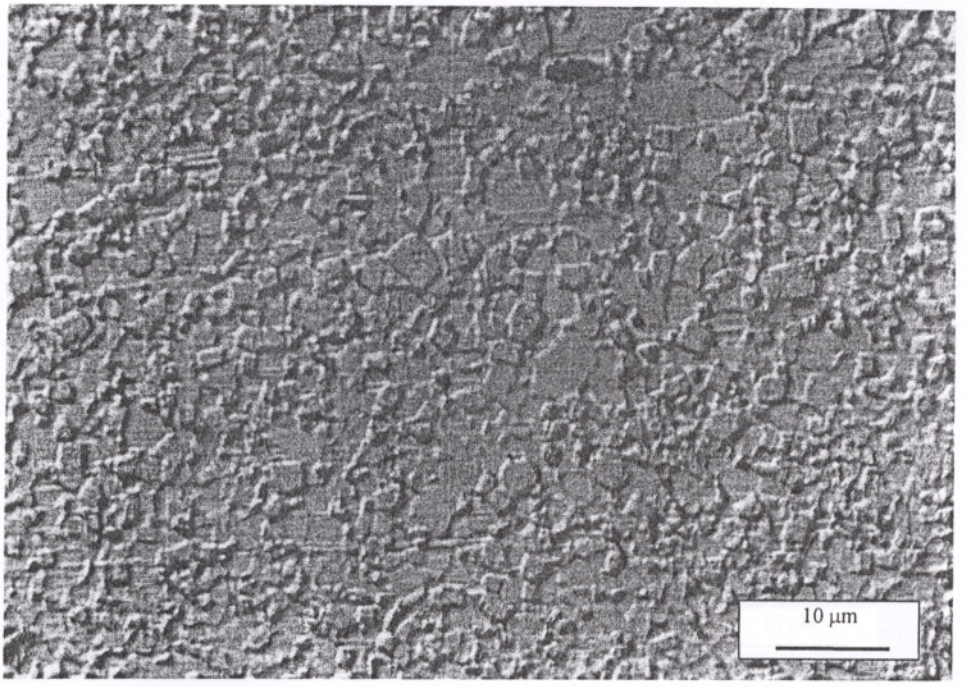

(a)

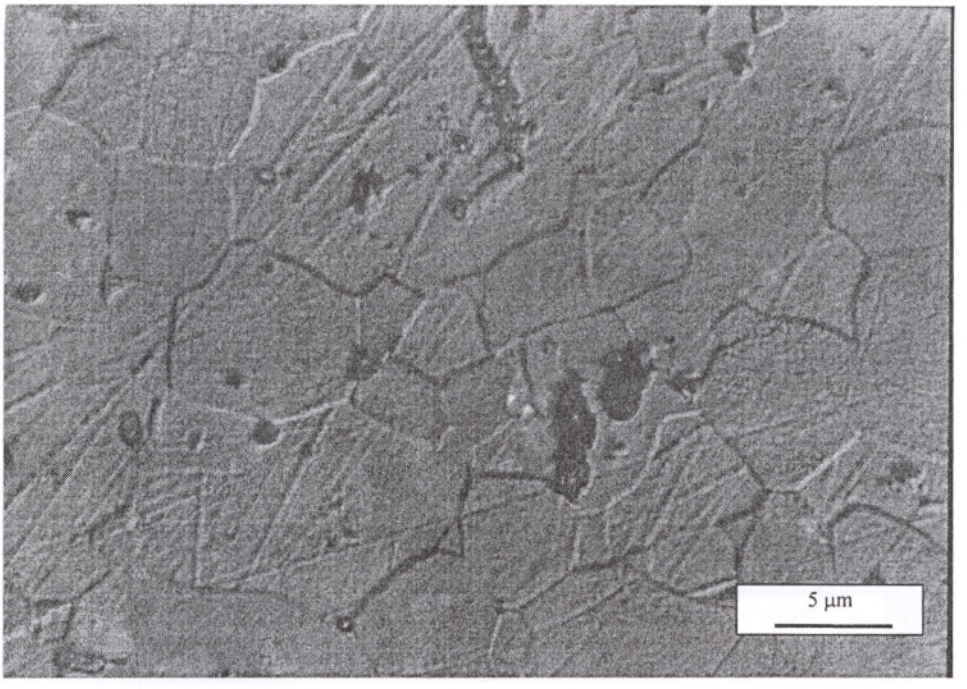

(b)

Figure 8.12. The photomicrographs of PCA100 powders at magnifications of , a) 750x, b)1500x

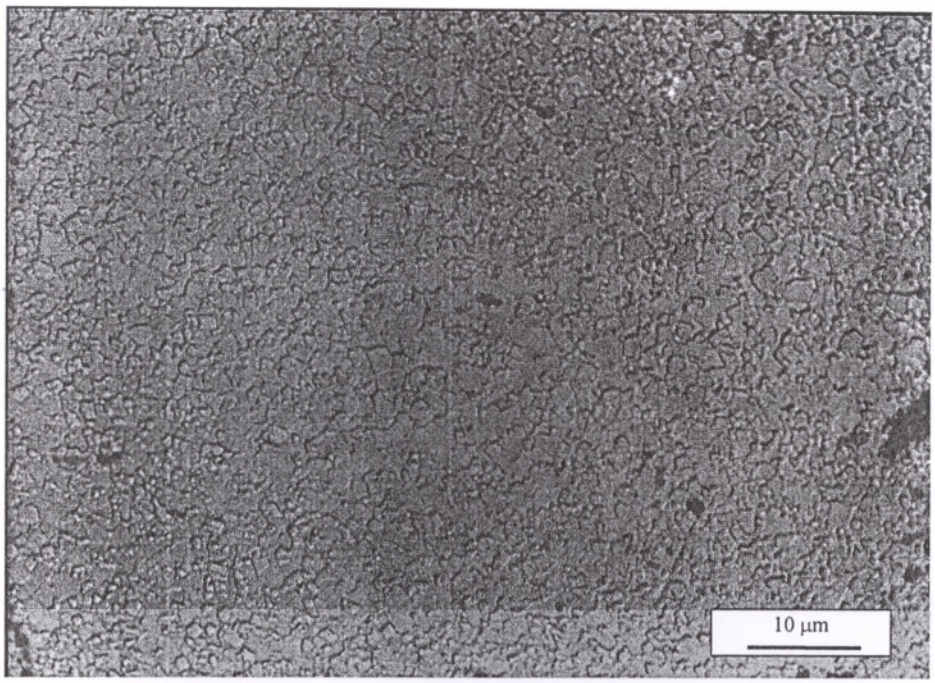

(a)

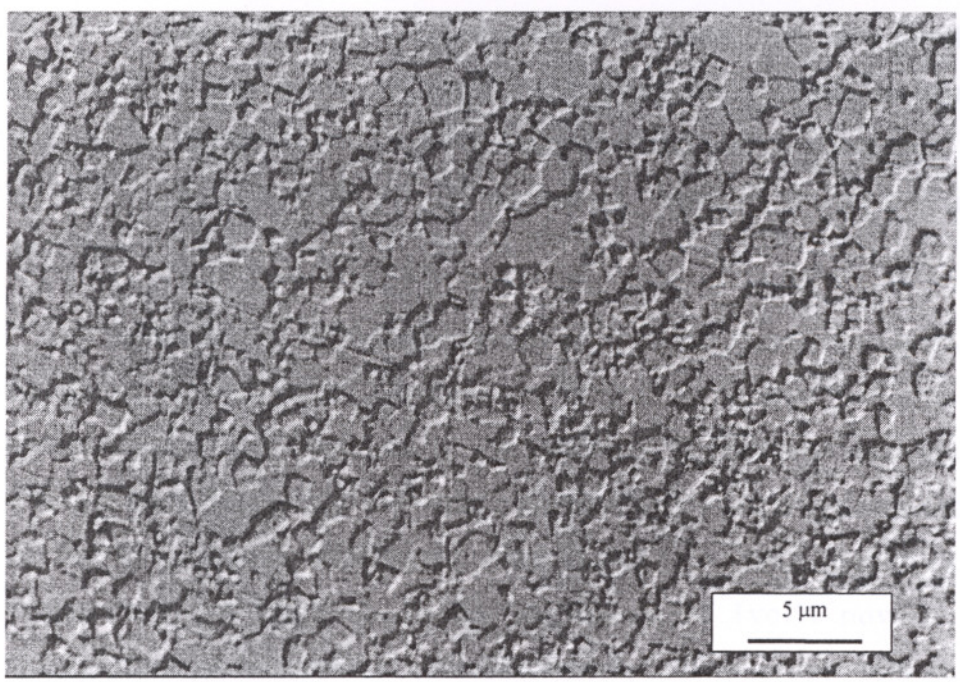

(b)

Figure 8.13. The photomicrographs of PCA50 powders at magnifications of , a) 750x, b)1500x

8.2.6 Rheological Measurements

The rheological measurements of $SrTiO_3$ powder dispersions in white oil were performed in order to investigate the effect of solids loading to the rheological properties of suspensions. The suspensions had 1, 5 and 10 vol% solids. In order to disperse the powders in white oil, a commercial oil dispersant (Chevron Chemicals, Oloa 1200- Ashless Succinimide Dispersant) was used. The amount of surfactant was 33 vol% of powder dispersed in oil.

As it can be seen in Figure 8.14, the viscosity of white oil without any solids did not show any changes with increasing shear rate as expected. Generally, oils show Newtonian behaviour. The relation between the shear rate and shear stress was linear as shown in Figure 8.15.

As it can be seen in Figures 8.16 and 8.17, 1 vol% $SrTiO_3$ suspension without surfactant behaved as a pseudoplastic fluid. The decrease in viscosity stands for the presence of flocculation within the suspension. The breakdown of flocs resulted in the release of liquid entrapped in the flocs decreasing the viscosity. The decrease in viscosity indicates that the suspensions were not stable. However, the addition of surfactant resulted in a well-dispersed suspension.

The addition of surfactant produced well-dispersed suspensions with approximately dilatant behaviour as it can be seen in Figures 8.18 and 8.19. No significant change was observed in the viscosity of fluid for well-dispersed 1 vol% suspension. The minor difference between the viscosities was most likely due to the temperature differences. The viscosity of well-dispersed 5 vol% suspension was not much above the suspension of 1vol% powder. 5 vol% suspension showed Newtonian behavior which indicates that this suspension was well-dispersed, thus stabilized as it can be seen in Figures 8.20 and 8.21. 10 vol% suspension stabilized with the same surfactant also showed the same behavior (Figures 8.22 and 8.23), however 3-fold increase in the viscosity of this suspension was observed.

Electrorheological experiment was performed with 10 vol% suspension. DC power supply was set to 1000 V, which corresponds to the electric field strength of 500 V/mm. However, DC power supply cut the field at 300 V/mm, most likely because of the fault in the set-up. In each attemp, the same problem was observed. Although the suspension showed no electrorheological effect, the particles were observed to be accumulated at the surface of the spindle, which corresponds to electrophoresis.

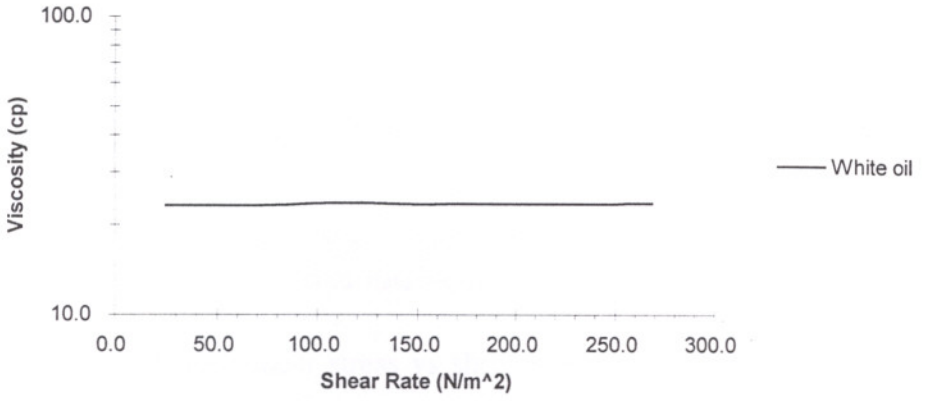

Figure 8.14. Change in viscosity of oil with respect to temperature.

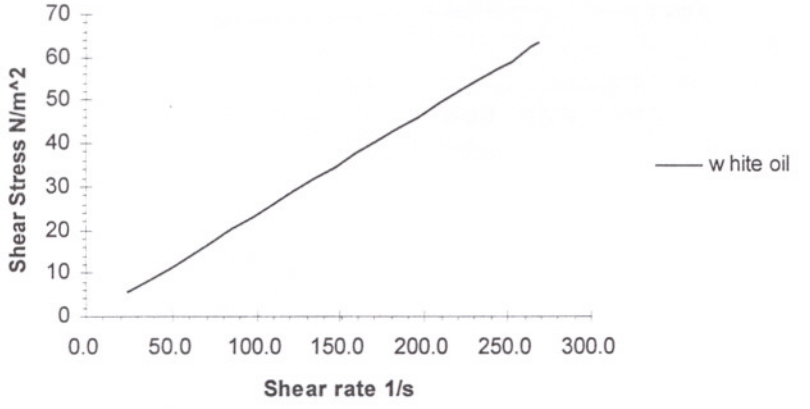

Figure 8.15. Plot of shear stress vs. shear rate for white-oil.

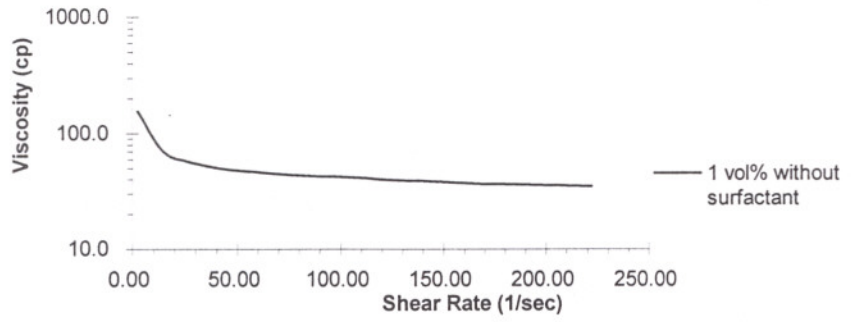

Figure 8.16. Change in viscosity of 1 vol % $SrTiO_3$ suspension with respect to shear rate (without surfactant).

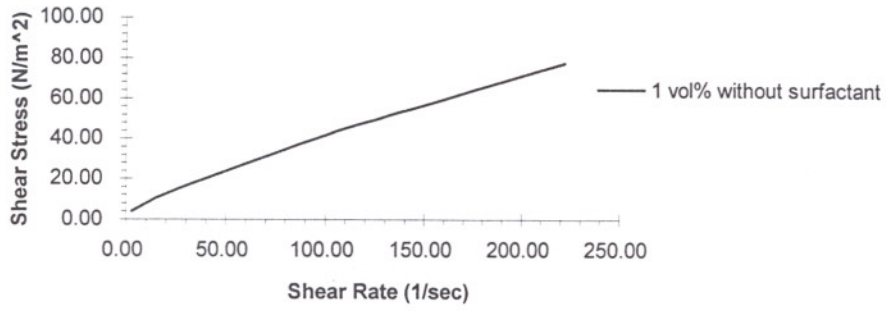

Figure 8.17. Plot of shear stress vs shear rate for 1 vol% $SrTiO_3$ suspension (without surfactant).

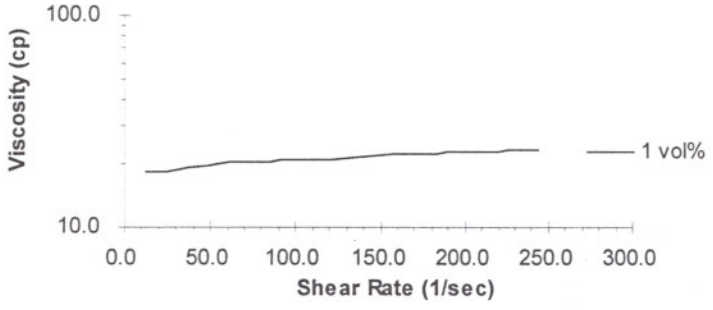

Figure 8.18. Change in the viscosity of 1 vol% $SrTiO_3$ suspension with respect to shear rate (with surfactant).

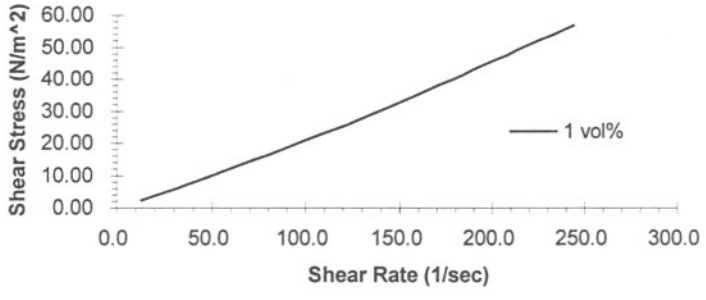

Figure 8.19. Plot of shear stress vs shear rate for 1 vol% $SrTiO_3$ suspension (with surfactant).

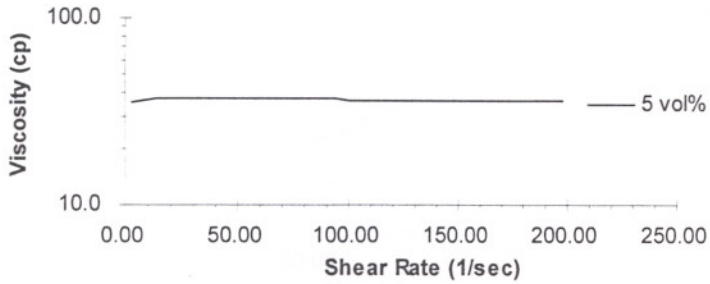

Figure 8.20. Change in the viscosity of 5 vol% $SrTiO_3$ suspension with respect to shear rate (with surfactant).

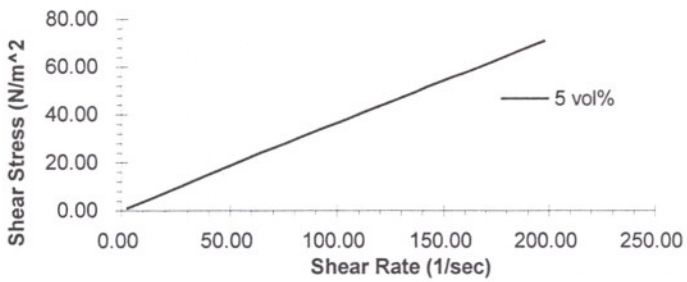

Figure 8.21. Plot of shear stress vs shear rate for 5 vol% $SrTiO_3$ suspension (with surfactant).

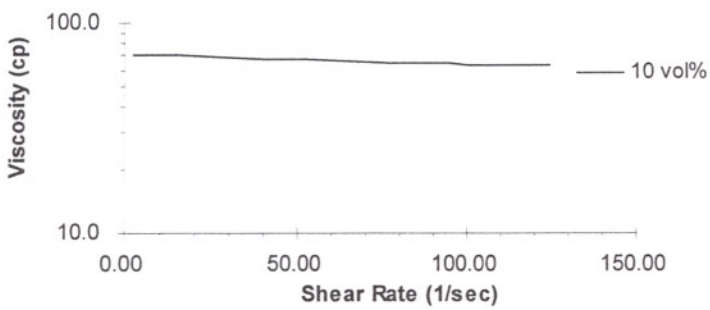

Figure 8.22. Change in the viscosity of 10 vol% $SrTiO_3$ suspension with respect to shear rate (with surfactant).

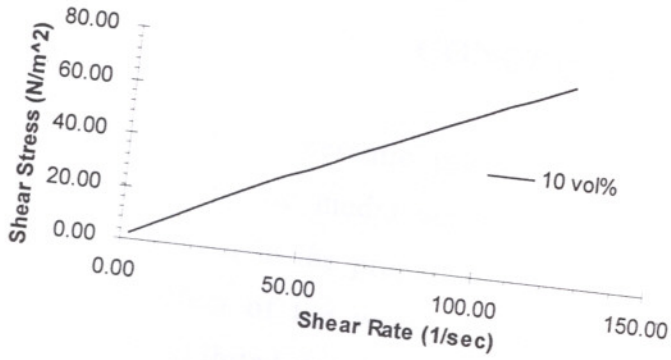

Figure 8.23. Plot of shear stress vs shear rate for 10 vol% $SrTiO_3$ suspension (with surfactant).

CONCLUSIONS

Preparation of ceramic powders and rheological behavior of powder dispersions in organic media were investigated in this work. Two chemical methods were used in the preparation of strontium titanate powder. In sol gel method, the effect of the water:alcohol:acid ratios was intestigated. Density measurement exhibited that the powder based on TC5 sol was more dense than that based on TC2 sols. However, the densities of sol-gel powders were much more less than the density of Pechini powders. Pechini powders have a density of well above 90%. The sol-gel powders had very strong agglomerates and sintered to very low densities.

The XRD analyses exhibited that $SrTiO_3$ phase was completely formed for Pechini powders except an additional SrO phase was found in the PCA50 powder. The 20 phases found in TC2 powder showed that calcination at 650 ^{0}C for 2 hours was not enough to form $SrTiO_3$ phase completely. Either the calcination temperature or the calcination time should be increased. However, FTIR spectra exhibited that calcination temperatures were high enough to remove the undesired chemicals. There were no additional peaks but peaks belonging to $SrTiO_3$.

The particle diameter of Pechini powders were in the range of 0.2-0.5 μm. The microstructural analyses showed that the grain size distribution of Pechini powders was more uniform than that of the sol-gel powders. The sintered Pechini pellets were crack-free but cracks and pores were observed on the surface of sol-gel derived pellets.

In the rheological experiments, the pseudoplastic behavior was observed for powder dispersions without surfactant. However, addition of surfactant produced well-dispersed, stabilized suspension. The increase in the solids loading did not change the viscosity of well-dispersed suspension significantly.

RECOMMENDATIONS

Future research following to this study may include:

1. Investigation of different acid:alcohol ratios on the morphology of sol-gel powder.

2. Investigation of the calcination temperature and time for sol-gel powder.

3. Formulation of strontium titanate powder suspension in different oils, and investigation of the effect of different surfactants on the stability of suspension.

4. Investigation of the electrorheological behaviour of strontium titanate suspensions with respect to the change in electric field, type of electric field and at different solids loading.

REFERENCES

[1]. Block, H., Electrorheological fluids; *Chemtech* June 1992, 368-373.

[2]. Block, H.; Kelly, J.P.; Review Articles: Electrorheology; *J. Phys. D: App. Phys.* 21(1998) 1661-1677.

[3]. Bowen C.P., Bhalla A.S., Newnham R.E., Randall C.A., An investigation of the assembly of the conditions of dielectric particles in uncured thermoset polymers, *J. Mater. Res.*, Vol. 9, No: 3, 1994, 781-788.

[4]. Budd K.D., Payne D.A., Preparation of Strontium Titanate Ceramics and Internal Boundary Layer Capacitors by the Pechini Method, *Mat. Res. Soc. Symp.*, Vol. 32 (1984), 239-244.

[5]. Caglar, Ozlem; The Preparation, Characterization of Sintering Behavior of Nanocrystalline Ceramics, M.Sc. Thesis, Materials Science and Engineering Department, Izmir Institute of Technology, 1999.

[6]. Ceramic and Glasses, *Engineered Materials Handbook*; ASM International, vol 4. 1991.

[7]. Chang, H.Y., Liu, K.S.; Conventional microwave sintering studies of $SrTiO_3$; *J. Mater. Res.* Vol:10 No:8 Aug 1995 2052-2059.

[8]. Cho S.G., Johnson P.F.; Evolution of the microstructure of undoped and Nb-doped $SrTiO_3$., *Journal of Materials Science*, 29, (1994), 4866-4874.

[9]. Cho, S.G., Johnson, P.F., Condrate, R.A.; Thermal decomposition of (Sr, Ti) organic precursors during the Pechini process; *Journal of Mat. Sci.* 25 (1990) 4738-4744.

[10]. Colthup, N.B., Daly, L.H., Wiberley, S.E.; *Introduction to Infrared and Raman Spectroscopy*, Academic Press, 2nd edition, 1990.

[11]. Conrad, H, Sprecher, A.F.; Characteristics and Mechanism of ER fluids; *Journal of Physics*; Vol: 64 no:5/6 1991, 1073-1091

[12]. Conrad, Hans; properties and design of ER suspensions; *MRS bulletin* Aug 1998, 35-42.

[13]. Fan, W., Niinistö, L; Preparation of Strontium Titanate Using Strontium Titanyl Oxalate as Precursor, *Materials Research Bulletin*, Vol:29 No:4 451-458.

[14]. Fujimoto M., Kingery W.D., Microstructures of $SrTiO_3$ Internal Boundary Layer Capacitors During and After Processing and Resultant Electrical Properties, *J. of the American Ceramic Society,* Vol:68, No:4, 1985, 169-173.

[15]. Gast, A.P.; Zukoski, C.F.; ER fluids as colloidal suspensions, *Advances in Colloid and Interface science*; 30(1989) 153-202.

[16]. Gilbert, S.R., Wessels, B.W., Marks, T.J.; Epitaxial growth of SrTiO3 thin films by metalorganic chemical vapor deposition, *Applied physics letters*, JUN 12 1995 v 66 n 24, 3298.

[17]. Gow, C.J.; Zukoski, C.F.; The Electrorheological properties of Polyaniline suspensions; *Journal of Colloid and Interface Sci*, Vol:136 No:1 (1990) 175-188.

[18]. Halsey, T.C., Electrorheological fluids, *Science*, Vol:258, 30 oct 1992, 761-766

[19]. Hanks R.W., *Materials Engineering Scince:An Introduction*, Harcourt, Brace & World, Inc. 1970.

[20]. Havelka, K.O.; Pialet, J.W.; ER technology: The future is now, *Chemtech*, June 1996, 36-45

[21]. Jo, K.H.; Yoon, K.K.; Preparation of sol-gel derived $(Ba_{0.2}Pb_{0.8})TiO_3$ powders; *Mat. Res. Bull.*, Vol:24, pp1-9; 1989.

[22]. Jordan, T.C., Shaw, M.T.; Electrorheology; *MRS bulletin*, Aug 1991 39-42

[23]. Jordan, Theresa C.; Shaw, M.T.; Electrorheology, *IEEE transactions an Electrical Insulation* Vol:24 No:5 October 1989 849-878.

[24]. Kakihana M., Arima M., Yashima M., Yoshimora M., Nakamura Y., Mazaki H. and Yasuoka H.; Polymerized complex route to the synthesis of multicomponent oxides, *Sol-Gel Science and Technology*, 65-76.

[25]. Kasap, S. O., *Principles of Electrical Engineering Materials and Devices*, McGraw-Hill, 1997.

[26]. Lee I. Burtland, Pope, J.A. Edward; *Chemical Processing of Ceramics*, Marcel Dekker, Inc. 1994, New York.

[27]. Lessing Paul A.; Mixed cation oxide powders via polymeric precursors; *Ceramic Bulletin*, vol:68, no:5 1989.

[28]. Livage, J., Sanchez C., Sol-gel chemistry, *Journal of Non-Crystalline solids* 145 (1992) 11-19.

[29]. P.W. Cahn, P. Haasen, E.J. Kramer, Material Science and Technology Vol:17 A, *Processing of Ceramics, part 1*, 1996.

[30]. Pampuch R., *Constitution and Properties of Ceramic Materials*, Polish Scientific Publishers, Warsawa 1991.

[31]. Paulson, A. Bradley; Use of sol-gels in the application of thin films of $BaTiO_3$, $LiNbO_3$, $LiTO_3$, Ph.D. Thesis March 1986.

[32]. Peschke, Steven L., Characterization of $SrTiO_3$ Powder produced by Polymeric Precursor, M.S. Thesis, Materials Engineering, New Mexico Institute of Mining and Technology, June 1991.

[33]. Princeton Scientific Corporation: Strontium Titanate, URL:http://www.princesci.com/crystal/stroti.html.

[34]. Reed, J.S., *Principles of Ceramics Processing*, John Wiley and Sons, Inc., 2nd edition, Canada,1995

[35]. Richerson, W. David; *Modern Ceramic Engineering*, Marcel Dekker Inc.; 1992, New York.

[36]. Sacks, Michael D., Rheological Science in Ceramic Processing, *Science of Ceramic Chemical Processing*, John Wiley and Sons, 1986, p. 523-538.

[37]. Smith J.S., Dolloff R.T., Mazdiyasni K.S.,.; Preparation and Characterization of Alkoxy derived $SrZrO_3$ and $SrTiO_3$, *J. Am. Cer. Soc.* Vol:53, 91-95.

[38]. Smith W.S., Foundations of Materials Science and Engineering, McGraw-Hill, Inc., Singapore, 1993.

[39]. Stangroom, J.E., Basic considerations in Flowing ER fluids; *Journal of Statistical Physics*, Vol:64, No:5/6 1991, 1059-1072.

[40]. The Materials Science of Field-Responsive Fluids, *MRS Bulletin*, August 1998, p. -21

[41]. Van Vlack, Lawrence H., *Elements of Materials Science and Engineering*, Addison-Wesley Publishing Company, 6th edition, 1989.

[42]. Varma, H.K., Pillai, P.K., Mani T.U.; Warrier, K.G.K, Damedoren A.D.; Spray Drying of Metal Alkoxide Sol for $SrTiO_3$ Ceramics, *J.Am. Cer. Soc.*; 77(1) 129-32; 1994.

[43]. Vinogradov, G.V., Deinega Y.F.; Electric Fields in the Rheology of Disperse Systems; *Rheologica acta*; 23:636-651, 1984.

[44]. Williams, R.A., *Colloid and Surface Engineering*, Butterword-Heinemann Ltd., Great Britain, 1992.

[45]. Wilson G. and Patel A; Recent Advances in Sol-gel processing for improved materials synthesis, *Materials science and technology* nov; vol:9 937-944.

[46]. Yang, W.D., Kao, C.F., Preparation and electrical properties of fine $SrTiO_3$ powder from titanium alkoxide in a strong alkaline solution, *Materials Sci. and eng. B*; 1996, 127-137.

[47]. Zhang, Y., Ma Y., Lan Y., Lu K., Liu W.; The Electrorheological behavior of complex strontium titanate suspensions, *Applied Physics Letter*, Vol. 73, No:10, 1998, 1326-1328.

[48]. Zukoski, C.F.; Material Properties and the Electrorheological response; Annu. *Rev. Mater. Sci.* 1993 23:45-78